Networks and Heterogeneous Media

https://www.aimspress.com/journal/nhm

NHM, 20(3): 903–937.
DOI: 10.3934/nhm.2025039
Received: 05 November 2024
Revised: 25 July 2025
Accepted: 05 August 2025
Published: 20 August 2025

Research article

Steady state blended gas flow on networks: Existence and uniqueness of solutions

Alena Ulke[1], **Michael Schuster**[2] **and Simone Göttlich**[1,*]

[1] Department of Mathematics, University of Mannheim, B6, 28-29, 68159 Mannheim, Germany

[2] Friedrich-Alexander University Erlangen-Nürnberg, Department of Mathematics, Cauerstraße 11, 91058 Erlangen, Germany

* **Correspondence:** Email: goettlich@uni-mannheim.de.

Abstract: We prove an existence result for the steady-state flow of gas mixtures in networks. The model is based on the physical principles of the isothermal Euler equations, coupling conditions for the flow and pressure, and the mixing of incoming flows at the nodes. The state equation is based on a convex combination of the ideal gas equations of state for natural gas and hydrogen. We analyze the mathematical properties of the model, allowing us to prove the existence of solutions for tree-shaped networks and networks with a cycle. Numerical examples illustrate the challenges involved, when extending our approach to general network topologies.

Keywords: gas pipeline network; gas mixture; hydrogen blending; isothermal Euler equations; stationary states

Nomenclature

Graph and Network Notation

$\mathcal{G} = (\mathcal{V}, \mathcal{E})$	Directed, connected graph with the nodes $v \in \mathcal{V}$ and edges $e \in \mathcal{E}$
$\mathcal{G}_{\text{flow}} = (\mathcal{V}, \mathcal{E}_{\text{flow}})$	Graph with the edges corresponding to the flow direction
$(C, \mathcal{E}_C)$	Subgraph of $\mathcal{G}$ that only the cycle of the graph $\mathcal{G}$
$(\mathcal{P}, \mathcal{E}_{\mathcal{P}})$	Subgraph of $\mathcal{G}$ that contains only the path between two nodes
$(\mathcal{P}(v), \mathcal{E}_{\mathcal{P}(v)})$	Path from a supply node v_0 to an arbitrary node v
$(\mathcal{P}(v, w), \mathcal{E}_{\mathcal{P}(v,w)})$	Path from a node v to a node w

$f(e) \in \mathcal{V}$	Foot or start node of edge e
$h(e) \in \mathcal{V}$	Head or end node of edge e
$w_e = w_e(v) \in \mathcal{V}$	Node of edge e that is not $v \in \{f(e), h(e)\}$
$\mathcal{V}_{<0} \subseteq \mathcal{V}$	Set of supply nodes
$\mathcal{V}_{\geq 0} \subseteq \mathcal{V}$	Set of demand nodes
$\mathcal{E}_+(v) \subseteq \mathcal{E}$	Set of incoming edges of node v
$\mathcal{E}_-(v) \subseteq \mathcal{E}$	Set of outgoing edges of node v
$\mathcal{E}(v) \subseteq \mathcal{E}$	Set of edges incident to node v
$A \in \mathbb{R}^{\lvert\mathcal{V}\rvert \times \lvert\mathcal{E}\rvert}$	Incidence matrix of a graph $\mathcal{G}$ with entries $a(v, e)$
$A_{-v} \in \mathbb{R}^{\lvert\mathcal{V}\rvert - 1 \times \lvert\mathcal{E}\rvert}$	The incidence matrix but without row v
$\boldsymbol{a}_v \in \mathbb{R}^{\lvert\mathcal{E}\rvert}$	Row v of the incidence matrix A
$A^{\mathcal{P}} \in \mathbb{R}^{\lvert\mathcal{P}\rvert \times \lvert\mathcal{E}_{\mathcal{P}}\rvert}$	Incidence matrix of the subgraph $(\mathcal{P}, \mathcal{E}_{\mathcal{P}})$
Variables of the Gas Flow Model	
$\rho_{\mathrm{NG},e}$	Density of natural gas in pipe e
$\rho_{\mathrm{H}_2,e}$	Density of hydrogen in pipe e
ρ_e	Density of gas mixture in pipe e
$q_{\mathrm{NG},e}$	Flow of natural gas in pipe e
$q_{\mathrm{H}_2,e}$	Flow of hydrogen in pipe e
q_e	Flow of gas mixture in pipe e
$\boldsymbol{q} \in \mathbb{R}^{\lvert\mathcal{E}\rvert}$	Flow vector with entries q_e
$\boldsymbol{q}^{\mathcal{P}} \in \mathbb{R}^{\lvert\mathcal{E}_{\mathcal{P}}\rvert}$	Flow vector on the subgraph $(\mathcal{P}, \mathcal{E}_{\mathcal{P}})$ with entries q_e
η_e	Mass fraction of hydrogen along pipe e
$\boldsymbol{\eta} \in \mathbb{R}^{\lvert\mathcal{E}\rvert}$	Composition vector with entries η_e
η_v	Mass fraction of hydrogen at node v
p_e	Pressure in the gas mixture in pipe e
p_v	Pressure in the gas mixture at node v
$\boldsymbol{p} \in \mathbb{R}^{\lvert\mathcal{V}\rvert}$	Nodal pressure vector with entries p_v
$\pi_e = p_e^2$	Potential along pipe e
$\pi_v = p_v^2$	Potential at node v

$\boldsymbol{\pi} \in \mathbb{R}^{\lvert\mathcal{V}\rvert}$	Nodal potential vector with entries π_v
$\boldsymbol{\pi}_{-v} \in \mathbb{R}^{\lvert\mathcal{V}\rvert-1}$	Nodal potential vector without entry π_v
b_v	Load of the node v
$\boldsymbol{b} \in \mathbb{R}^{\lvert\mathcal{V}\rvert}$	Load vector with entries b_v
$\boldsymbol{b}^{\mathcal{P}} \in \mathbb{R}^{\lvert\mathcal{P}\rvert}$	Modified load vector on the subgraph $(\mathcal{P}, \mathcal{E}_{\mathcal{P}})$ with entries $b_v^{\mathcal{P}}$
ζ_v	Mass fraction of the supply at node v
σ^2_{NG}	Sound speed in natural gas
$\sigma^2_{\mathrm{H_2}}$	Sound speed in hydrogen
$R_{S,\mathrm{NG}}$	Specific gas constant for natural gas
$R_{S,\mathrm{H_2}}$	Specific gas constant for hydrogen
T	Gas temperature
L_e	Pipe length of pipe e
D_e, D	Diameter of pipe e
λ_{Fr}	Friction factor
Cut Graph and the Existence Result	
$\mathcal{G}^c = (\mathcal{V}^c, \mathcal{E}^c)$	Cut graph corresponding to graph $\mathcal{G}$ and the cut edge e^c
v_{cl}, $v_{\mathrm{cr}} \in \mathcal{V}^c$	New nodes generated by cutting the edge e^c
e_{cl}, $e_{\mathrm{cr}} \in \mathcal{E}^c$	New edges generated by cutting the edge e^c
c	Superscript to indicated that variables correspond to the cut graph $\mathcal{G}^c$
λ	Flow through the cut edge e^c
μ	Mass fraction through the cut edge e^c
$H_p(\lambda, \mu)$	Difference between the squared pressure at v_{cl} and v_{cr}
$H_\eta(\lambda, \mu)$	Difference between the mass fraction at v_{cl} and at v_{cr}
$\mu_\eta(\lambda)$	Root curve of H_η such that $H_\eta(\lambda, \mu_\eta(\lambda)) = 0$
$g(\lambda) = H_p(\lambda, \mu_\eta(\lambda))$	Restriction of H_p to the root curve μ_η
γ_e	Root of the flow q_e^c on the cut graph G^c with respect to λ for $e \in \mathcal{E}_C \setminus \{e^c\}$
$\gamma_{\min}$	Minimum of all roots γ_e
$\gamma_{\max}$	Maximum of all roots γ_e

1. Introduction

The transition to renewable energy is one of the most intensely discussed topics in science, and hydrogen is a key element that is expected to play an increasingly important role in the global energy mix. Hydrogen offers numerous advantages. Firstly, it is a clean energy source that can be produced using renewable energy sources such as wind and solar power, and its combustion results only in water and heat [1, 2]. Secondly, hydrogen can be utilized to decarbonize sectors that are difficult to electrify, such as heavy industry [1, 2]. Lastly, hydrogen serves as an energy carrier, making it a valuable resource for energy storage [2, 3]. Given these benefits, there is no doubt that hydrogen will play an important role in the near future.

However, the transition to renewable energies necessitates not only an appreciation of hydrogen's clean-energy potential but also a deep understanding of how to integrate it into current energy systems. Even if hydrogen transport networks are planned all over the world (cf. [4] for Europe, [5] for Asia, and [6] for the United States), hydrogen is far from completely replacing natural gas as energy source. One key strategy to reduce the use of natural gas as energy source as well as to significantly lower the amount of emitted greenhouse gases is the blending of hydrogen into natural gas networks.

A rigorous mathematical understanding of the hydrogen-natural gas blending processes is essential for the efficiency and safety of existing pipeline networks. In comparison with the transport of pure hydrogen, the complexity lies in the modeling and understanding of the mixing of two gases. While the transport of pure hydrogen as well as pure natural gas in pipeline networks can be modeled by isothermal Euler equations, cf. [7–9], a different approach is needed for the modeling of gas mixtures. Since natural gas has been and still is widely used as an energy source almost all over the world, researchers can rely on well-established regulations for natural gas networks and extensive research in this area. In [10], the authors discuss the stationary states of the isothermal Euler equations, and in [11], the existence of unique stationary states was shown on arbitrary graphs. In [7, 12], the authors analyze the transient model and discuss solutions to Riemann problems on arbitrary graphs including appropriate coupling conditions at the nodes, that is, conservation of mass and pressure continuity. Furthermore, the existence of semi-global Lipschitz continuous solutions of isothermal Euler equations on a network with compatible coupling conditions was shown in [13], based on a fixed-point iteration along the characteristic curves for Lipschitz continuous initial and boundary conditions. While the modeling of gas networks usually relies on one-dimensional consideration along pipes, we also emphasise that network models for flows in two space dimensions are available, see, for instance, [14–16].

However, applying the isothermal Euler equations for both hydrogen and natural gas in the same pipeline does not consider collisions of molecules of different types, which leads to adulterated results [17]. On the basis of an analysis of chemically reacting fluid mixtures in [18, 19], we consider a model for the flow of a natural gas and hydrogen mixture under perfect mixing conditions (i.e., both gases have the same velocity and temperature). In a pipe with length $L > 0$, for $(t, x) \in [0, t_{\text{final}}] \times [0, L]$, the mixing model is given by

$$\partial_t \rho_{\text{NG}}(t,x) + \partial_x q_{\text{NG}}(t,x) = 0, \tag{1.1a}$$

$$\partial_t \rho_{\text{H}_2}(t,x) + \partial_x q_{\text{H}_2}(t,x) = 0, \tag{1.1b}$$

$$\partial_t q(t,x) + \partial_x \left[p(\rho_{\text{NG}}(t,x), \rho_{\text{H}_2}(t,x)) + \frac{q^2(t,x)}{\rho(t,x)} \right] = -\frac{\lambda_{\text{Fr}}}{2D} \frac{q(t,x)|q(t,x)|}{\rho(t,x)}, \tag{1.1c}$$

where ρ_{NG} and ρ_{H_2} are the densities of natural gas and hydrogen, respectively; q_{NG} and q_{H_2} are the flows of natural gas and hydrogen, respectively; and $\rho = \rho_{NG} + \rho_{H_2}$ and $q = q_{NG} + q_{H_2}$ are the density and the flow of the mixing, respectively. $\lambda_{Fr} > 0$ is the pipe friction coefficient and $D > 0$ the pipe diameter. The pressure $p(\rho_{NG}, \rho_{H_2})$ of the mixture depends on the densities of the gases. It is given by a state equation for the gas mixture, derived, for example, in [20] for a mixture of ideal gases and in [21] for a mixture of real gases. The latter also assumes non-isothermal dynamics.

The mixing model (1.1) in networks also includes coupling conditions at the network junctions. For the transport of natural gas in networks, depending on the physical properties of the gas, conservation of mass and continuity of pressure are common choices, cf. [11, 22–24]. In [12], the authors give an overview about the coupling conditions for models of natural gas transport in networks. In the mixing model (1.1), we also consider perfect mixing at the nodes, which implies that the outgoing hydrogen concentration is equal to the average weighted by the flow of all ingoing concentrations.

For long-time-horizon planning of gas networks, dynamic models are often replaced by static models that represent the steady states, cf. [10, 11, 17, 22, 24]. Simulation results for models based on Eq (1.1) and the corresponding steady-state models were presented, for example, in [17, 25, 26]. Considering natural gas and hydrogen as ideal gases, in [27], the authors present a well-posedness result of Eq (1.1) under the assumption that the hydrogen concentration is sufficiently low. To our best knowledge, neither the existence of steady states for the mixing model (1.1) nor steady states for the mixing on networks has been theoretically analyzed yet. The only result that fits into this line of research is that for tree-shaped networks, steady-state solutions are unique if they exist (cf. [17]). However, proving uniqueness becomes more complex for networks with cycles, since the monotonicity of the pressure, which guarantees the uniqueness for pure natural gas transport, is unclear a priori due to the mixing.

In this paper, we present an explicit solution of the steady states of Eq (1.1). Further, we analyze the existence and uniqueness of steady states for the hydrogen-blended natural gas flow in networks. We discuss tree-shaped pipeline networks as well as networks that contain cycles. For pure gas flow, the existence and uniqueness of steady states was analyzed in [11] for ideal gases and in [28] for real gases. In the case of gas mixtures, the gas composition in a pipeline depends on the direction of the flow, which leads to discontinuities in the mixing model if the graph contains cycles. Thus, due to the discontinuity, the strategy applied in [11, 28] to show the existence and uniqueness of steady states cannot be applied for gas mixtures. We present a novel existence result for the steady states of the mixing model for networks with a cycle. The result is based on a cutting edge approach, such that the existence of a solution is shown in the resulting tree-shaped network with new supply and demand nodes. The main challenge arises from the discontinuities in the gas composition at the new supply and demand nodes, highlighting the increased complexity compared to pure natural gas networks, where such discontinuities do not occur.

The article is structured as follows: First, we introduce and motivate the gas flow model for mixtures in networks in Section 2. We show that certain properties of the gas flow of a single gas also hold for the mixture model. In Section 3, we establish the existence of steady-state solutions for tree-shaped networks and networks with a single cycle. Finally, in Section 4, we present a numerical study on the extension of our approach to networks with arbitrary cycles and on the uniqueness of the solutions.

2. The model equations in networks

In this section, we derive a steady-state model for the hydrogen-blended natural gas flow in pipeline networks. We further define suitable boundary and coupling conditions for the flow, the pressure, and the composition of the gas mixture at the junctions of the network.

Let $\mathcal{G} = (\mathcal{V}, \mathcal{E})$ be a connected, directed graph with a set of nodes $\mathcal{V}$ and a set of edges $\mathcal{E} \subseteq \mathcal{V} \times \mathcal{V}$. Each edge e represents a pipe of length L_e, and each node v represents a network junction. Let $\mathcal{V}_{<0}$ be the set of *inflow* (supply) nodes where gas enters the network, and let $\mathcal{V}_{\geq 0}$ be the set of outflow (demand) nodes where gas leaves the network. We have $\mathcal{V} = \mathcal{V}_{<0} \cup \mathcal{V}_{\geq 0}$ with $\mathcal{V}_{<0} \cap \mathcal{V}_{\geq 0} = \emptyset$. For every node $v \in \mathcal{V}$, the sets of *incoming* and *outgoing edges* are given by

$$\mathcal{E}_-(v) := \{e \in \mathcal{E} \mid e = (\bullet, v)\} \quad \text{and} \quad \mathcal{E}_+(v) := \{e \in \mathcal{E} \mid e = (v, \bullet)\},$$

respectively. For an edge $e \in \mathcal{E}_-(v)$, the node v is their *head* or *end node*, and for an edge $e \in \mathcal{E}_+(v)$, the node $v \in \mathcal{V}$ is their *foot* or *start node*. The set $\mathcal{E}(v) = \mathcal{E}_-(v) \cup \mathcal{E}_+(v)$ contains all edges connected to node v. In the following, we denote the head of an edge by $h(e)$ and the foot of an edge by $f(e)$, i.e., we have

$$e = (v, w) \quad \Leftrightarrow \quad f(e) = v \quad \text{and} \quad h(e) = w.$$

Further, let $A \in \mathbb{R}^{|\mathcal{V}| \times |\mathcal{E}|}$ be the *node edge incidence matrix*, whose entries are defined by

$$a(v, e) := \begin{cases} -1, & \text{if } v = f(e), \text{ i.e., } v \text{ is the start node of } e, \\ 1, & \text{if } v = h(e), \text{ i.e., } v \text{ is the end node of } e, \\ 0, & \text{otherwise.} \end{cases} \tag{2.1}$$

2.1. The isothermal Euler equations for mixtures

For the flow of hydrogen-blended natural gas through a pipeline $e \in \mathcal{E}$, we consider the stationary states corresponding to the transient model (1.1). Since the gas velocity is small compared with the speed of sound, the term q_e^2/ρ_e in the transient model (1.1) is neglectable (see, e.g., [8, 11]). Thus, the subsonic steady-state hydrogen blended gas flow model is given by

$$\partial_x q_{\mathrm{NG},e}(x) = 0, \qquad \text{for } x \in [0, L_e] \tag{2.2a}$$

$$\partial_x q_{\mathrm{H_2},e}(x) = 0, \qquad \text{for } x \in [0, L_e] \tag{2.2b}$$

$$\partial_x p_e(\rho_{\mathrm{NG},e}(x), \rho_{\mathrm{H_2},e}(x)) = -\frac{\lambda_{\mathrm{Fr}}}{2D} \frac{q_e(x)|q_e(x)|}{\rho_e(x)}, \qquad \text{for } x \in [0, L_e] \tag{2.2c}$$

where $\rho_{\mathrm{NG},e}$ and $\rho_{\mathrm{H_2},e}$ denote the density, and $q_{\mathrm{NG},e}$ and $q_{\mathrm{H_2},e}$ the flow of natural gas and hydrogen along the pipe, respectively. The constant $\lambda_{\mathrm{Fr}} > 0$ denotes the pipe friction, and D is the diameter of the pipe. For the reader's convenience, we assume the same friction and diameter for every pipe. Moreover, ρ_e is the density, q_e is the flow, η_e is the composition, and p_e is the pressure of the gas mixture along the pipe $e \in \mathcal{E}$. These quantities are defined as

$$\rho_e(x) = \rho_{\mathrm{H_2},e}(x) + \rho_{\mathrm{NG},e}(x), \quad q_e(x) = q_{\mathrm{H_2},e}(x) + q_{\mathrm{NG},e}(x), \quad \eta_e(x) = \frac{q_{\mathrm{H_2},e}(x)}{q_e(x)} = \frac{\rho_{\mathrm{H_2},e}(x)}{\rho_e(x)},$$

while the latter holds due to the perfect mixing assumption, i.e., both gases have the same velocity. Considering ideal gases, the state equation for the gas mixture is given by a convex combination of the state equations of the single gases [20]; i.e., we have

$$p_e(\rho_{\mathrm{NG},e}(x), \rho_{\mathrm{H}_2,e}(x)) = \left[\eta_e(x)\sigma_{\mathrm{H}_2}^2 + (1-\eta_e(x))\sigma_{\mathrm{NG}}^2\right]\rho_e(x), \tag{2.3}$$

where $\sigma_{\mathrm{H}_2}^2 = R_{S,\mathrm{H}_2}T$ is the speed of sound in hydrogen and $\sigma_{\mathrm{NG}}^2 = R_{S,\mathrm{NG}}T$ is the speed of sound in natural gas. Moreover, R_{S,H_2} and $R_{S,\mathrm{NG}}$ are the specific gas constants of hydrogen and natural gas, respectively, and T is the temperature of the gas. Then, the solution to the mixture model (2.2) is given by

$$q_{\mathrm{NG},e}(x) = \text{const}, \quad q_{\mathrm{H}_2,e}(x) = \text{const}, \tag{2.4a}$$

$$p_e^2(x) = p_e^2(0) - \frac{\lambda_{\mathrm{Fr}}}{D}\left(\eta_e\sigma_{\mathrm{H}_2}^2 + (1-\eta_e)\sigma_{\mathrm{NG}}^2\right)q_e|q_e|x. \tag{2.4b}$$

The flows of hydrogen and natural gas are constant along the pipe and the pressure profile is uniquely defined by the pressure at the beginning and the end of the pipe.

Remark 2.1. If the right-hand-side of Eq (2.4b) is non-negative for all $x \in [0, L_e]$, the pressure profile is given by

$$p_e(x) = \sqrt{p_e^2(0) - \frac{\lambda_{\mathrm{Fr}}}{D}\left(\eta_e\sigma_{\mathrm{H}_2}^2 + (1-\eta_e)\sigma_{\mathrm{NG}}^2\right)q_e|q_e|x}.$$

This is true when the initial pressure $p_e(0)$ is larger than a critical threshold $p_{\mathrm{crit},e}$ or when the pipes are shorter than a critical length $L_{\mathrm{crit},e}$. Otherwise, the pressure profile $p_e(x)$ is undefined in $\mathbb{R}$. For a given pipe length L_e, the critical pressure is given by:

$$p_{\mathrm{crit},e} = \sqrt{\max\left\{0, \frac{\lambda_{\mathrm{Fr}}}{D}\left(\eta_e\sigma_{\mathrm{H}_2}^2 + (1-\eta_e)\sigma_{\mathrm{NG}}^2\right)q_e|q_e|L_e\right\}}, \tag{2.5}$$

and for a given initial pressure, the critical length, in the case that $q_e > 0$, is given by:

$$L_{\mathrm{crit},e} = \frac{p_e^2(0)}{\frac{\lambda_{\mathrm{Fr}}}{D}\left(\eta_e\sigma_{\mathrm{H}_2}^2 + (1-\eta_e)\sigma_{\mathrm{NG}}^2\right)q_e^2}. \tag{2.6}$$

If $q_e \leq 0$, there is no restriction on the pipe length as the gas flows from the end $x = L_e$ to the beginning $x = 0$ of the pipe, i.e., we have $p_e(L_e) \geq p_e(0) \geq 0$.

Introducing the potential $\pi_e = p_e^2$ allows us to express Eq (2.4) in terms of π_e. The mixture model (2.2) has a solution in terms of π_e that is independent of the boundary data. In the case where $\pi_e \geq 0$, the pressure profile is given by $p_e(x) = \sqrt{\pi_e(x)}$. Otherwise, the corresponding pressure is physically infeasible, making such solutions, including the boundary data, physically irrelevant. For better readability, we omit the dependence of the variable x in the following.

2.2. Boundary and coupling conditions for the nodes

As gas enters or leaves the network at the nodes, we introduce the load vector $\boldsymbol{b} \in \mathbb{R}^{|\mathcal{V}|}$ given by

$$b_v \begin{cases} < 0 & \text{if } v \in \mathcal{V}_{<0}, \text{ which means } v \text{ is a supply node,} \\ \geq 0 & \text{if } v \in \mathcal{V}_{\geq 0}, \text{ which means } v \text{ is a demand node.} \end{cases} \tag{2.7}$$

The case $b_v = 0$ implies, that gas is neither injected nor withdrawn from node v. For the boundary conditions, let the loads b_v be given at each node $v \in \mathcal{V}$ and let the supply compositions ζ_v be given at every supply node $v \in \mathcal{V}_{<0}$. Furthermore, let the pressure p^* be given at an arbitrary yet fixed node $v^* \in \mathcal{V}$, i.e., we set $p_{v^*} = p^*$.

For the coupling conditions, we make three assumptions to describe the gas flow across nodes. Firstly, the mass of the mixture and the mass of the individual gases are conserved. Secondly, the gas mixes perfectly and instantaneously. Lastly, the pressure is continuous across a node.

The first assumption, the conservation of mass at a node $v \in \mathcal{V}$ means that the amount of gas entering node v must be equal to the amount of gas leaving node v, including the supply and demand of the node, respectively; i.e., we have

$$\sum_{e \in \mathcal{E}_-(v)} q_e - \sum_{e \in \mathcal{E}_+(v)} q_e = b_v.$$

Using the incidence matrix A defined in Eq (2.1), the conservation of mass of the mixture at all nodes $v \in \mathcal{V}$ is given by

$$\sum_{e \in \mathcal{E}(v)} a(v,e) q_e = b_v \quad \text{for all} \quad v \in \mathcal{V} \qquad \Leftrightarrow \qquad A\boldsymbol{q} = \boldsymbol{b}, \tag{2.8}$$

where $\boldsymbol{q} \in \mathbb{R}^{|\mathcal{E}|}$ is the vector of (constant) flows at the edges.

Remark 2.2. Due to the conservation of mass and the definition of the incidence matrix A, the loads b_v must sum up to zero, i.e., we have

$$\sum_{v \in \mathcal{V}} b_v = 0. \tag{2.9}$$

Hence, it is sufficient to provide the loads b_v for $|\mathcal{V}| - 1$ nodes, as the missing load is automatically determined by Eq (2.9).

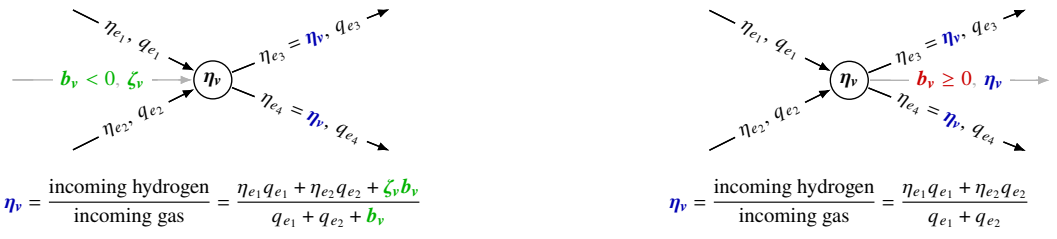

Figure 1. The mixing of gas for a supply node (left) and a demand node (right). The supply and demand of a node can be seen as an invisible pipe with a fixed flow.

Next, we discuss perfect mixing at the nodes, which implies that the incoming gas compositions at a node v are weighted by the respective incoming flows and then averaged. Thus, the composition of all outgoing flows is equal. Hence, we define the nodal composition η_v of the gas at a node $v \in \mathcal{V}$ by

$$\eta_v = \frac{\text{incoming hydrogen}}{\text{outgoing gas}} = \frac{\text{incoming hydrogen}}{\text{incoming gas}},$$

while the latter holds due to the conservation of mass. In Figure 1, we provide an example how to compute the nodal composition for a supply and a demand node.

As the flow direction might differ from the edge orientation, it is unclear a priori, which pipes transport incoming gas and which pipes transport outgoing gas. However, we can use the incidence matrix to determine whether a given flow q_e of an edge $e \in \mathcal{E}(v)$ is directed towards or away from the node v:

$$\begin{aligned} a(v,e)\, q_e \geq 0 \quad &\Leftrightarrow \quad \text{Gas in pipe } e \text{ flows towards node } v. \\ a(v,e)\, q_e \leq 0 \quad &\Leftrightarrow \quad \text{Gas in pipe } e \text{ flows away from } v. \end{aligned} \tag{2.10}$$

(a) The flow q_e is directed into a node v, i.e., an inflow, if and only if $a(v,e)q_e \geq 0$.

(b) The flow q_e is directed away from a node v, i.e., an outflow, if and only if $a(v,e)q_e \leq 0$.

Figure 2. The four possible relations between flow and edge direction, cf. Eq (2.10).

We provide a visualization of the condition (2.10) in Figure 2. For a number α, we define $\alpha^+ = \max\{\alpha, 0\}$ and $\alpha^- = \max\{-\alpha, 0\}$. Then, the nodal composition η_v is given by

$$\eta_v = \frac{\sum_{e\in\mathcal{E}(v)} \eta_e \cdot \left(a(v,e)q_e\right)^+ + \zeta_v b_v^-}{\sum_{e\in\mathcal{E}(v)} \left(a(v,e)q_e\right)^+ + b_v^-}, \tag{2.11}$$

where η_e is the composition in pipe e. There is an explicit relation between the nodal composition η_v and the composition in pipe η_e, since the nodal composition η_v is transferred to all pipes $e \in \mathcal{E}(v)$ transporting outgoing gas. More specifically, we have

$$\eta_e = \begin{cases} \eta_{f(e)} & \text{if } q_e \geq 0, \\ \eta_{h(e)} & \text{if } q_e < 0, \end{cases} \quad \text{for all} \quad e \in \mathcal{E}, \tag{2.12}$$

which means that the composition η_e is always given by the upstream nodal composition. Eq (2.12)

allows us to express Eq (2.11) fully in terms of nodal compositions, that is,

$$\eta_v = \frac{\sum_{e\in\mathcal{E}(v)} \eta_{w_e} \left(a(v,e)q_e\right)^+ + \zeta_v b_v^-}{\sum_{e\in\mathcal{E}(v)} \left(a(v,e)q_e\right)^+ + b_v^-} \quad \text{where} \quad w_e = \begin{cases} f(e), & \text{if } v = h(e), \\ h(e), & \text{if } v = f(e). \end{cases}$$

Lastly, we discuss the continuity of the pressure across a node. This means that all nodes $v \in \mathcal{V}$ and all incident edges $e, \tilde{e} \in \mathcal{E}(v)$ satisfy

$$p_e(x_e) = p_{\tilde{e}}(x_{\tilde{e}}) \quad \text{where} \quad x_e = \begin{cases} 0, & e \in \mathcal{E}_-(v), \\ L_e, & e \in \mathcal{E}_+(v). \end{cases}$$

As the pressure change along a pipe is defined by Eq (2.4), we ensure the continuity of the pressure across a node by introducing the nodal pressure p_v for each node v. Then, Eq (2.4) is given by

$$p_{h(e)}^2 - p_{f(e)}^2 = -\frac{\lambda_{\mathrm{Fr}}}{D}\left(\eta_e \sigma_{\mathrm{H_2}}^2 + (1-\eta_e)\sigma_{\mathrm{NG}}^2\right) q_e|q_e|L_e \quad \text{for all} \quad e \in \mathcal{E}.$$

As the composition η_e on an edge is discontinuous in $q_e = 0$ (cf. Eq (2.12)), the pressure p_e is discontinuous in $q_e = 0$ as well. However, for the transport of a single gas, the pressure continuously depends on the nodal pressure and on the gas flow; e.g., [28, 29]. Since the continuity is crucial for our further analysis, we express the pressure change in terms of the nodal composition instead of the composition at the edges. First, we have

$$\eta_e \sigma_{\mathrm{H_2}}^2 + (1-\eta_e)\sigma_{\mathrm{NG}}^2 = \frac{1}{2}\left(\frac{|q_e|}{q_e} + 1\right)\sigma(\eta_{f(e)}) - \frac{1}{2}\left(\frac{|q_e|}{q_e} - 1\right)\sigma(\eta_{h(e)}) \quad \text{for } e \in \mathcal{E},$$

where $\sigma(\eta_v) \coloneqq \eta_v \sigma_{\mathrm{H_2}}^2 + (1-\eta_v)\sigma_{\mathrm{NG}}^2$ for $v \in \mathcal{V}$. Then, for each edge $e \in \mathcal{E}$, we define

$$\tilde{\sigma}(\eta_{f(e)}, \eta_{h(e)}, q_e) \coloneqq -\frac{\lambda_{\mathrm{Fr}}}{D} L_e \left[\frac{1}{2}\left(\frac{|q_e|}{q_e} + 1\right)\sigma(\eta_{f(e)}) - \frac{1}{2}\left(\frac{|q_e|}{q_e} - 1\right)\sigma(\eta_{h(e)})\right], \tag{2.13}$$

which allows us to derive an expression for the pressure change along a pipe in terms of the nodal compositions with removable singularity

$$p_{h(e)}^2 - p_{f(e)}^2 = \tilde{\sigma}(\eta_{f(e)}, \eta_{h(e)}, q_e) q_e|q_e| \quad \text{for all} \quad e \in \mathcal{E}. \tag{2.14}$$

2.3. The full model on graphs

The full steady-state model for gas mixtures consists of the pressure change along the pipes, the pressure continuity at the nodes, the conservation of mass at the nodes, the mixing of the gases at the nodes, and suitable boundary conditions. For each node $v \in \mathcal{V}$, let a load b_v be given with $\sum_{v\in\mathcal{V}} b_v = 0$.

Further, let the supply compositions ζ_v be given at each supply node $v \in \mathcal{V}_{<0}$, let a nodal pressure $p_{v^*} = p^*$ be given at an arbitrary node $v^* \in \mathcal{V}$. For these boundary conditions, the gas mixture model is given by

$$p_{h(e)}^2 - p_{f(e)}^2 = \tilde{\sigma}(\eta_{f(e)}, \eta_{h(e)}, q_e) q_e |q_e| \qquad \text{for all } e = (f(e), h(e)) \in \mathcal{E}, \tag{2.15a}$$

$$A\boldsymbol{q} = \boldsymbol{b} \qquad \text{for all } v \in \mathcal{V}, \tag{2.15b}$$

$$\eta_v = \frac{\sum_{e \in \mathcal{E}(v)} \eta_e \cdot (a(v,e) q_e)^+ + \zeta_v b_v^-}{\sum_{e \in \mathcal{E}(v)} (a(v,e) q_e)^+ + b_v^-} \qquad \text{for all } v \in \mathcal{V}. \tag{2.15c}$$

Remark 2.3. As in Remark 2.1, we introduce the nodal potential $\pi_v = p_v^2$ and solve the mixing model (2.15) in the variables (π_v, q_e, η_v). If $\pi_v \geq 0$, the nodal pressures p_v are given by the roots of the nodal potential, which strongly depends on the boundary data, c.f., Remark 2.1. Hence, we will discuss both the existence of nodal potentials and the existence of nodal pressures.

2.4. Properties of the gas flow

Considering single-gas transport, the gas cannot flow in cycles without compressor stations [11]. This also holds for gas mixtures and is essential for showing the existence of solutions for the mixture model (2.15). We prove this by determining the pressure change along a path, since a cycle is a path with identical start and end.

Lemma 2.4 (Pressure change along a path)**.** *Let $\mathcal{G} = (\mathcal{V}, \mathcal{E})$ be a graph and let $(\mathcal{P}, \mathcal{E}_\mathcal{P})$ be a path from v_0 to v_k where $\mathcal{P} = \{v_0, \dots, v_k\}$. The set $\mathcal{E}_\mathcal{P}$ contains the edges connecting two consecutive nodes v_i and v_{i+1}. Then the pressure change along the path is given by*

$$p_{v_k}^2 - p_{v_0}^2 = \sum_{e \in \mathcal{E}_\mathcal{P}} \tilde{\sigma}(\eta_{h(e)}, \eta_{f(e)}, q_e) a(v_e, e) q_e |a(v_e, e) q_e|,$$

where v_e is the node of edge e that is closer to the start node v_0 of the path, i.e., $v_e = f(e)$ if $e = (v_i, v_{i+1})$ and $v_e = h(e)$ if $e = (v_{i+1}, v_i)$.

Proof. We rewrite the pressure change between two consecutive nodes v_i and v_{i+1} of the path, i.e., the pressure change along the pipe connecting v_i and v_{i+1}:

$$\begin{aligned}
p_{v_{i+1}}^2 &= \begin{cases} p_{v_i}^2 - \tilde{\sigma}(\eta_{v_i}, \eta_{v_{i+1}}, q_e) q_e |q_e|, & \text{if } e = (v_i, v_{i+1}) \\ p_{v_i}^2 + \tilde{\sigma}(\eta_{v_{i+1}}, \eta_{v_i}, q_e) q_e |q_e|, & \text{if } e = (v_{i+1}, v_i) \end{cases} \\
&= \begin{cases} p_{v_i}^2 + \tilde{\sigma}(\eta_{f(e)}, \eta_{h(e)}, q_e) a(v_i, e) q_e |a(v_i, e) q_e|, & \text{if } e = (v_i, v_{i+1}) \\ p_{v_i}^2 + \tilde{\sigma}(\eta_{f(e)}, \eta_{h(e)}, q_e) a(v_{i+1}, e) q_e |a(v_{i+1}, e) q_e|, & \text{if } e = (v_{i+1}, v_i) \end{cases} \\
&= p_{v_i}^2 + \tilde{\sigma}(\eta_{f(e)}, \eta_{h(e)}, q_e) a(v_e, e) q_e |a(v_e, e) q_e|.
\end{aligned}$$

Then, the claim follows by an induction over the path length $|\mathcal{E}_\mathcal{P}|$.

Gas flowing in a cycle means that the gas always flows either away from or into the node when traversing through the cycle, starting from an arbitrary, designated start node. Thus, we use Eq (2.10) to characterize circular flows and obtain the following corollary.

Corollary 2.5. *Let $\mathcal{G} = (\mathcal{V}, \mathcal{E})$ be a graph. Then a solution to the gas flow model* (2.15) *cannot contain circular flows, i.e., there is no cycle $(C, \mathcal{E}_C)$ satisfying one of the following two conditions:*

(i) $a(v_e, e)\, q_e \geq 0$ *for all* $e \in \mathcal{E}_C$ *and* $a(v_e, e)\, q_e > 0$ *for at least one* $e \in \mathcal{E}_C$,

(ii) $a(v_e, e)\, q_e \leq 0$ *for all* $e \in \mathcal{E}_C$ *and* $a(v_e, e)\, q_e < 0$ *for at least one* $e \in \mathcal{E}_C$,

where $v_e \in \mathcal{V}$ is incident to e and the node closest to the start node while ignoring the start-end edge (cf. Lemma 2.4).

Proof. We use proof by contradiction to show the first case (i). A cycle $(C, \mathcal{E}_C)$ is a path with identical start and end. Thus, applying Lemma 2.4 yields:

$$0 = p_{v_k}^2 - p_{v_0}^2 = \sum_{e \in \mathcal{E}_C} \underbrace{\tilde{\sigma}\left(\eta_{f(e)}, \eta_{h(e)}, q_e\right)}_{\geq 0} \underbrace{a(v_e, e) q_e}_{\geq 0} \underbrace{|a(v_e, e) q_e|}_{\geq 0} \overset{(*)}{>} 0,$$

which is a contradiction. The strict inequality $(*)$ holds because there is at least one edge $e \in \mathcal{E}_C$ satisfying $a(v_e, e) q_e > 0$. The proof for the second case (ii) follows analogously, and the corollary is proven.

3. The existence and uniqueness of steady states in networks

In this section, we prove the existence of steady states for the mixture model (2.15) on networks. The idea follows [28, 29], where the authors prove the existence of steady states on networks for the gas flow model for a single gas. Their proof is based on induction over the number of cycles in a graph. To apply the induction assumption, they cut an edge of a cycle to obtain a graph with one cycle less than the original one.

Thus, we first show the existence and uniqueness of solutions of the mixture model (2.15) on tree-shaped networks, i.e., a network with no cycles, and establish the existence of steady states for networks with cycles afterwards.

3.1. Steady states on tree-shaped networks

The existence and uniqueness of steady states for tree-shaped networks is similar to the single gas problem, as the argument only relies on the fact, that for trees, the flow on the network is fully determined by the loads b_v. However, the mixing model additionally contains the equation for the mixing at the nodes.

Since the nodal composition η_v is given by the ratio of incoming hydrogen and incoming mixed gas (cf. Eq (2.15c)), we can compute the composition η_v at a node v, if we know its incoming flows and their compositions. As the network is tree-shaped, we can sort the nodes such that gas always flows from nodes early in the ordering to nodes later in the ordering, which allows us to compute the nodal compositions η_v in an inductive manner. Such an ordering of the nodes is called a *topological ordering* of a graph.

Definition 3.1 (Topological ordering [30])**.** Let $\mathcal{G} = (\mathcal{V}, \mathcal{E})$ be a tree-shaped graph. Then a *topological ordering* sorts the nodes of the graph into a sequence in which, for each directed edge (v, w), the start node v appears before the end node w (c.f., Figure 3 for a visualization).

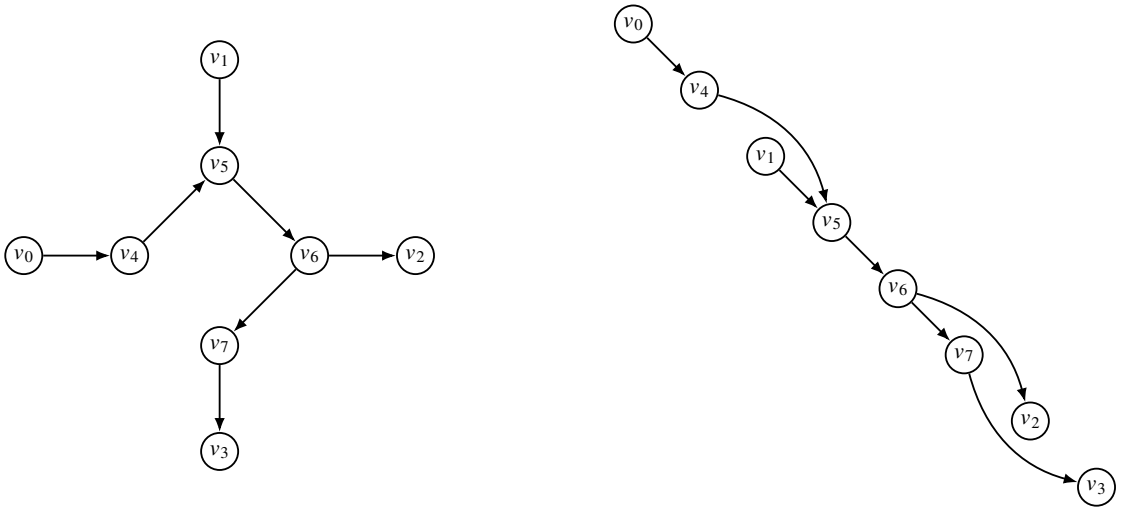

Figure 3. A directed acyclic graph (left) and a topological ordering of its nodes (right).

To compute the compositions η_v for fixed flows q_e, we require a topological ordering of the graph $\mathcal{G}_{\text{flow}} = (\mathcal{V}, \mathcal{E}_{\text{flow}})$, which has the same nodes as $\mathcal{G}$ but edges according to the flow direction, i.e., its edges are defined by

$$(v, w) \in \mathcal{E}_{\text{flow}} \quad :\Leftrightarrow \quad \begin{cases} (v, w) \in \mathcal{E}, & \text{if } q_e \geq 0, \\ (w, v) \in \mathcal{E}, & \text{if } q_e < 0. \end{cases} \tag{3.1}$$

A topological ordering of the graph $\mathcal{G}$, based on its original edge orientations, does not necessarily reflect the actual direction of gas flow, since flow can oppose the edge orientation. As a result, gas may flow from nodes later in the ordering to nodes that are earlier, which is not desirable for analysis. In contrast, a topological ordering of the flow-oriented graph $\mathcal{G}_{\text{flow}}$, where the edges are aligned with the actual direction of flow, ensures that gas consistently flows from earlier to later nodes in the ordering.

Note that the graph $\mathcal{G}_{\text{flow}}$ emerges from the original graph $\mathcal{G}$ by flipping edges where the flow and edge direction differ. Hence, the graph $\mathcal{G}_{\text{flow}}$ depends on the flow q_e on the edges.

Remark 3.2. The graph $\mathcal{G}_{\text{flow}}$ is tree-shaped because it has the same edges as $\mathcal{G}$ up to a change in the edge orientation and thus, by [30, Proposition 2.1.3], a topological ordering of the nodes of $\mathcal{G}_{\text{flow}}$ exists.

The next lemma states the existence of a solution for the mixing Eq (2.15c) for given flows q_e on a network:

Lemma 3.3 (Existence of the composition)**.** *Let $\mathcal{G} = (\mathcal{V}, \mathcal{E})$ be a graph and let q_e be the flows at the edges satisfying mass conservation (cf. Eq (2.15b)). Then the mixing Eq* (2.15c) *has at least one solution η_v.*

Proof. The graph $\mathcal{G}_{\text{flow}} = (\mathcal{V}, \mathcal{E}_{\text{flow}})$ is acyclic. Thus, a topological ordering of the nodes of $\mathcal{G}_{\text{flow}}$ exists, and we can compute the nodal compositions η_v by induction over the position k in the topological ordering.

The composition η_v for the node at position $k = 1$ is given by the boundary data, since the first node in a topological ordering is a supply node, i.e., $b_v < 0$, where $a(v, e)q_e \leq 0$ for all $e \in \mathcal{E}(v)$, and thus $\eta_v = \zeta_v$.

Assume, that all nodal compositions up to position k have been determined. Then we compute the composition of the node at position $k+1$ by

$$\eta_v = \frac{\sum_{e\in\mathcal{E}(v)} \eta_e \cdot (a(v,e)q_e)^+ + \zeta_v b_v^-}{\sum_{e\in\mathcal{E}(v)} (a(v,e)q_e)^+ + b_v^-}.$$

The incoming flow, i.e., edges with $(a(v,e)q_e)^+ \neq 0$, is given only by the previous nodes in the ordering; otherwise an edge whose end point is before its start point in the ordering exists, which is a contradiction to the definition of a topological order. Thus, the composition for the node at position $k+1$ can be computed and the lemma is proven.

The proof of the existence of a solution relies on a topological ordering of the nodes. Even though the topological ordering is, in general, non-unique, we can show the uniqueness of the composition in the following lemma.

Lemma 3.4 (Uniqueness of the composition)**.** *Let $\mathcal{G} = (\mathcal{V}, \mathcal{E})$ be a tree-shaped graph and let q_e be an flows at the edges satisfying the mass conservation (cf. Eq (2.15b)). Then the solution η_v of the mixing Eq* (2.15c) *is unique.*

Proof. The claim follows directly from the proof by contradiction in [17, Theorem 1]. Considering a non-unique solution, tracing back to a supply node, where the composition is given by fixed boundary data, yields a contradiction.

Finally, we prove the existence and uniqueness of a solution of the steady-state gas flow model (2.15) for tree-shaped networks.

Theorem 3.5 (Existence of solutions for tree-shaped networks)**.** *Let $\mathcal{G} = (\mathcal{V}, \mathcal{E})$ be a tree-shaped network. Then there are unique vectors $(\boldsymbol{\pi}, \boldsymbol{q}, \boldsymbol{\eta}) \in \mathbb{R}^{|\mathcal{V}|} \times \mathbb{R}^{|\mathcal{E}|} \times [0,1]^{|\mathcal{V}|}$ satisfying the mixture model* (2.15) *with $\boldsymbol{\pi} = \boldsymbol{p}^2$. If $\boldsymbol{\pi} \geq 0$, then $(\boldsymbol{p}, \boldsymbol{q}, \boldsymbol{\eta}) \in \mathbb{R}^{|\mathcal{V}|} \times \mathbb{R}^{|\mathcal{E}|} \times [0,1]^{|\mathcal{V}|}$ is the unique solution of the mixture model* (2.15) *with $\boldsymbol{p} = \sqrt{\boldsymbol{\pi}}$.*

Proof. As the network $\mathcal{G}$ is tree-shaped, the incidence matrix A has full column rank [31, Lemma 2.2], and thus the flow equation $A\boldsymbol{q} = \boldsymbol{b}$ has a unique solution if and only if

$$\sum_{v\in\mathcal{V}} b_v = 0.$$

Since this holds by assumption, the flow equation has a unique solution $\boldsymbol{q}$ that only depends on the loads and the topology of the tree. Hence, by Lemmas 3.3 and 3.4, the mixing Eq (2.15c) has a unique solution.

Together with the fixed nodal pressure p_v at the node v^* and the relation $\pi_v = p_v^2$, we rewrite Eq (2.15a), which describes the pressure change along the pipes, using the incidence matrix. This yields the linear system

$$A^\top \boldsymbol{\pi} = \tilde{\boldsymbol{\sigma}}(\boldsymbol{\eta}, \boldsymbol{q}) \quad \text{with} \quad \pi_{v^*} = \pi^* = (p^*)^2 \tag{3.2a}$$

$$\Leftrightarrow \qquad A_{-v^*}^\top \boldsymbol{\pi}_{-v^*} = \underbrace{\tilde{\boldsymbol{\sigma}}(\boldsymbol{\eta}, \boldsymbol{q}) - \pi^* \boldsymbol{a}_{v^*}}_{\text{fully determined}}, \tag{3.2b}$$

where A_{-v^*} and $\boldsymbol{\pi}_{-v^*}$ are the incidence matrix A and the vector $\boldsymbol{\pi}$, but without the row and entry corresponding to v^*, respectively; $\boldsymbol{a}_{v^*}$ denotes the row of A corresponding to v^*. Moreover, the function $\tilde{\boldsymbol{\sigma}}$ is the vector value with the entries

$$[\tilde{\boldsymbol{\sigma}}(\boldsymbol{\eta}, \boldsymbol{q})]_e = \tilde{\sigma}(\eta_{f(e)}, \eta_{h(e)}, q_e),$$

where $\tilde{\sigma}$ is defined in Eq (2.13). Then we obtain the nodal potentials π_v by solving the linear system (3.2b), as the right side of this linear system is fully determined by the topology of the tree, the flow q_e, the composition η_e on the edges, and the given nodal pressure at node v^*. Moreover, the square matrix $A_{-v^*}^\top$ is regular, cf. [32], which completes the proof.

Note that Theorem 3.5 only guarantees the existence of the nodal potentials $\boldsymbol{\pi} \in \mathbb{R}^{|\mathcal{V}|}$, but not necessarily the existence of the nodal pressures $\boldsymbol{p} \in \mathbb{R}^{|\mathcal{V}|}$. For a single edge, the critical pressure and the critical length defined in Eqs (2.5) and (2.6) guarantee the existence of the nodal pressure at the end of the pipe. For networks, the existence of nodal pressures strongly depends on the graph topology. However, for tree-shaped networks, the flow is given a priori by the solution of $A\boldsymbol{q} = \boldsymbol{b}$, which allows us to provide sufficient conditions for the existence of nodal pressures. For a tree with a single supply node, we can formulate the following lemma.

Lemma 3.6. *Let $\mathcal{G} = (\mathcal{V}, \mathcal{E})$ be a tree-shaped graph with a single supply node v_0, where the flow direction meets the edge orientation for every edge $e \in \mathcal{E}$. Let $(\mathcal{P}(v), \mathcal{E}_{\mathcal{P}(v)})$ be the unique path from v_0 to an arbitrary node $v \in \mathcal{V}$. Assume that the condition*

$$p_{v^*}^2 \;\geq\; \frac{\lambda_{\mathrm{Fr}}}{D}\left(\zeta_{v_0}\sigma_{\mathrm{H_2}}^2 + (1-\zeta_{v_0})\sigma_{\mathrm{NG}}^2\right)\left[\sum_{e\in\mathcal{E}_{\mathcal{P}(w)}} q_e^2 L_e - \sum_{e\in\mathcal{E}_{\mathcal{P}(v^*)}} q_e^2 L_e\right],$$

holds for all nodes $w \in \mathcal{V}$ with $\mathcal{E}_+(w) = \emptyset$, then unique nodal pressures $\boldsymbol{p} \in \mathbb{R}^{|\mathcal{V}|}$ exist.

The statement of Lemma 3.6 is both sufficient and necessary. It is based on following the pressure change from the only supply node v_0 to any end node. Note that even if $\mathcal{G}$ does not satisfy the compatibility between the flow direction and the edge orientation, Eq (3.6) holds for the graph $\mathcal{G}_{\mathrm{flow}} = (\mathcal{V}, \mathcal{E}_{\mathrm{flow}})$ defined in Eq (3.1).

Proof of Lemma 3.6. We apply Lemma 2.4 to determine the pressure change between the supply node v_0 and the node v^*, where the pressure is given through boundary data:

$$p_{v_0}^2 = p_{v^*}^2 - \sum_{e\in\mathcal{E}_{\mathcal{P}(v^*)}} \tilde{\sigma}(\eta_{f(e)}, \eta_{h(e)}, q_e) q_e|q_e|.$$

Due to graph being tree-structured with only a single supply node, the composition at every edge is equal to the supply composition ζ_{v_0} and the flow direction given a priori meets the edge orientation for every edge, and thus we can replace η_e by ζ_{v_0} and $q_e|q_e|$ by q_e^2 and obtain

$$p_{v_0}^2 = p_{v^*}^2 + \frac{\lambda_{\mathrm{Fr}}}{D}\left(\zeta_{v_0}\sigma_{\mathrm{H_2}}^2 + (1-\zeta_{v_0})\sigma_{\mathrm{NG}}^2\right)\sum_{e\in\mathcal{E}_{\mathcal{P}(v^*)}} q_e^2 L_e. \tag{3.3}$$

As the pressure profiles are decreasing along every path, it is sufficient to consider only the end nodes of the graph, i.e., the nodes without outgoing edges. Using Lemma 2.4 again together with Eq (3.3), we can express the pressure at a node $w \in \mathcal{V}$ with $\mathcal{E}_+(w) = \emptyset$ by

$$\begin{aligned} p_w^2 &= p_{v_0}^2 - \frac{\lambda_{\mathrm{Fr}}}{D}\left(\zeta_{v_0}\sigma_{\mathrm{H}_2}^2 + (1-\zeta_{v_0})\sigma_{\mathrm{NG}}^2\right) \sum_{e\in\mathcal{E}_{\mathcal{P}(w)}} q_e^2 L_e, \\ &= p_{v^*}^2 + \frac{\lambda_{\mathrm{Fr}}}{D}\left(\zeta_{v_0}\sigma_{\mathrm{H}_2}^2 + (1-\zeta_{v_0})\sigma_{\mathrm{NG}}^2\right) \sum_{e\in\mathcal{E}_{\mathcal{P}(v^*)}} q_e^2 L_e \\ &\quad - \frac{\lambda_{\mathrm{Fr}}}{D}\left(\zeta_{v_0}\sigma_{\mathrm{H}_2}^2 + (1-\zeta_{v_0})\sigma_{\mathrm{NG}}^2\right) \sum_{e\in\mathcal{E}_{\mathcal{P}(w)}} q_e^2 L_e. \end{aligned}$$

The nodal pressure p_w exists, if p_w^2 is non-negative, which is the case if and only if

$$p_{v^*}^2 \;\geq\; \frac{\lambda_{\mathrm{Fr}}}{D}\left(\zeta_{v_0}\sigma_{\mathrm{H}_2}^2 + (1-\zeta_{v_0})\sigma_{\mathrm{NG}}^2\right)\left[\sum_{e\in\mathcal{E}_{\mathcal{P}(v^*)}} q_e^2 L_e - \sum_{e\in\mathcal{E}_{\mathcal{P}(w)}} q_e^2 L_e\right].$$

For tree-shaped graphs with an arbitrary number of supply nodes, we can neither replace η_e by ζ_{v_0} nor replace $q_e|q_e|$ by q_e^2. However, we can formulate a sufficient condition.

Corollary 3.7. *Let $\mathcal{G} = (\mathcal{V}, \mathcal{E})$ be a tree-shaped graph, where the flow direction meets the edge orientation for every edge $e \in \mathcal{E}$, and let $(\mathcal{P}(v,w), \mathcal{E}_{\mathcal{P}(v,w)})$ be the unique path from node v to node w. Further, set $\overline{\zeta} := \max\{\zeta_v \mid v \in \mathcal{V}_{<0}\}$ if $\sigma_{\mathrm{H}_2} \geq \sigma_{\mathrm{NG}}$ and $\overline{\zeta} := \min\{\zeta_v \mid v \in \mathcal{V}_{<0}\}$ if $\sigma_{\mathrm{H}_2} < \sigma_{\mathrm{NG}}$. If*

$$p_{v^*}^2 \;\geq\; \frac{\lambda_{\mathrm{Fr}}}{D}\left(\overline{\zeta}\sigma_{\mathrm{H}_2}^2 + (1-\overline{\zeta})\sigma_{\mathrm{NG}}^2\right)\left[\sum_{e\in\mathcal{E}_{\mathcal{P}(v,w)}} q_e|q_e|L_e - \sum_{e\in\mathcal{E}_{\mathcal{P}(v,v^*)}} q_e|q_e|L_e\right],$$

for all $v \in \mathcal{V}_{<0}$ and for all $w \in \mathcal{V}$ with $\mathcal{E}_+(w) = \emptyset$, then unique nodal pressures $\boldsymbol{p} \in \mathbb{R}^{|\mathcal{V}|}$ exist.

As in Lemma 3.6, even if $\mathcal{G}$ does not satisfy the compatibility between the flow direction and the edge orientation, Eq (3.7) holds for the graph $\mathcal{G}_{\mathrm{flow}} = (\mathcal{V}, \mathcal{E}_{\mathrm{flow}})$ defined in Eq (3.1).

3.2. Steady states in networks with one cycle

In this section, we discuss the existence of solutions to the mixture model (2.15) for networks with cycles. In particular, we prove the main result of Theorem 3.8, namely the existence of solutions for networks with a single cycle. Moreover, we also comment on whether the result extends to networks with active elements such as compressors.

Theorem 3.8 (Existence of solutions for networks with one cycle)**.** *Let $\mathcal{G} = (\mathcal{V}, \mathcal{E})$ be a graph with exactly one cycle. Then at least one tuple of vectors $(\boldsymbol{\pi}, \boldsymbol{q}, \boldsymbol{\eta}) \in \mathbb{R}^{|\mathcal{V}|} \times \mathbb{R}^{|\mathcal{E}|} \times [0,1]^{|\mathcal{V}|}$ exists with $\boldsymbol{\pi} = \boldsymbol{p}^2$ satisfying the mixture model* (2.15)*. If $\boldsymbol{\pi} \geq 0$, then $(\boldsymbol{p}, \boldsymbol{q}, \boldsymbol{\eta}) \in \mathbb{R}^{|\mathcal{V}|} \times \mathbb{R}^{|\mathcal{E}|} \times [0,1]^{|\mathcal{V}|}$ is a solution of the mixture model* (2.15) *with $\boldsymbol{p} = \sqrt{\boldsymbol{\pi}}$.*

Before we delve into the proof of Theorem 3.8, we discuss the sufficient conditions under which we can recover the nodal pressures p_v from the nodal potentials π_v. As for tree-shaped graphs, Theorem 3.8

only guarantees the existence of nodal potentials $\boldsymbol{\pi} \in \mathbb{R}^{|\mathcal{V}|}$, but not necessarily the existence of nodal pressures $\boldsymbol{p} \in \mathbb{R}^{|\mathcal{V}|}$. In contrast to tree-shaped graphs, we do not know the flows on the edges a priori, which makes it rather difficult to state sufficient conditions for the existence of nodal pressures. This problem is well-known in mathematics. In [33, Proposition 4], the authors present bounds on the nodal potentials as necessary conditions for a single gas flow model. In [11, 13], the authors state an existence result for the single gas model with sufficiently short pipes without also specifying the maximal pipe length. However, to state sufficient conditions for the existence of nodal pressures, we exploit the idea of Corollary 3.7 and follow the paths in the graph, considering the maximal possible pressure loss. The maximal possible flow $q_{\max}$ on an edge is given by the sum of all outflows as follows:

$$q_e \;\leq\; q_{\max} := \sum_{v \in \mathcal{V}_{\geq 0}} b_v \quad \text{for all} \quad e \in \mathcal{E}.$$

Since the paths between two arbitrary nodes $v, w \in \mathcal{V}$ might not be unique anymore, we define

$$\mathrm{P}(v,w) := \Big((\mathcal{P}_1(v,w), \mathcal{E}_{P_1(v,w)}), \cdots, (\mathcal{P}_d(v,w), \mathcal{E}_{P_d(v,w)}) \Big),$$

as the set of all cycle-free paths from $v \in \mathcal{V}$ to $w \in \mathcal{V}$. The number d of paths connecting the two nodes depends on v and w. As in Corollary 3.7, we set $\overline{\zeta} := \max\{\zeta_v \mid v \in \mathcal{V}_{<0}\}$ if $\sigma_{\mathrm{H}_2} \geq \sigma_{\mathrm{NG}}$, and $\overline{\zeta} := \min\{\zeta_v \mid v \in \mathcal{V}_{<0}\}$ if $\sigma_{\mathrm{H}_2} < \sigma_{\mathrm{NG}}$. Thus we have

$$|\tilde{\sigma}(\eta_{f(e)}, \eta_{h(e)}, q_e)| \leq \frac{\lambda_{\mathrm{Fr}}}{D} \Big(\overline{\zeta} \sigma_{\mathrm{H}_2}^2 + (1 - \overline{\zeta}) \sigma_{\mathrm{NG}}^2 \Big) L_e.$$

With that, we can state the following sufficient condition for the existence of nodal pressures.

Corollary 3.9. *Let $\mathcal{G} = (\mathcal{V}, \mathcal{E})$ be a graph with a single cycle. Assume that the following condition holds for all $w \in \mathcal{V}$ with $\mathcal{E}_+(w) = \emptyset$ and $i = 1, \cdots, d$:*

$$p_{v^*}^2 \;\geq\; \frac{\lambda_{\mathrm{Fr}}}{D} \Big(\overline{\zeta} \sigma_{\mathrm{H}_2}^2 + (1 - \overline{\zeta}) \sigma_{\mathrm{NG}}^2 \Big) \sum_{e \in \mathcal{E}_{\mathcal{P}_i(v^*,w)}} q_{\max}^2 L_e.$$

Then the nodal pressures $\boldsymbol{p} \in \mathbb{R}^{|\mathcal{V}|}$ exist.

The following corollary provides a weaker sufficient condition that is easier to verify:

Corollary 3.10. *Let the assumptions of Corollary 3.9 be satisfied. Furthermore, assume that the following conditions holds:*

$$p_{v^*}^2 \geq \frac{\lambda_{\mathrm{Fr}}}{D} \left(\overline{\zeta} \sigma_{\mathrm{H}_2}^2 + (1 - \overline{\zeta}) \sigma_{\mathrm{NG}}^2 \right) |\mathcal{E}|\, q_{\max}^2 \max_{e \in \mathcal{E}} L_e.$$

Then the nodal pressures $\boldsymbol{p} \in \mathbb{R}^{|\mathcal{V}|}$ exist.

In [34], the authors discuss the difference between a mathematical and a feasible (resp. physical) solution. They state that even if a solution in terms of negative nodal potentials (resp. complex nodal pressures) exists, the given boundary data does not provide a feasible solution, i.e., the solution does not meet physical properties. Thus, numerically, it is always beneficial to compute the nodal potentials

first, since they always exist.

Next, we discuss the proof of Theorem 3.8. The key idea to prove the existence of nodal potentials is to cut an edge of the cycle, which results in a tree-shaped network, for which we know that a unique solution exists (Theorem 3.5). The cut creates two new nodes that require boundary data, for which we introduce two parameters. As our aim is to show that the mixture model (2.15) admits a solution, we derive additional constraints that a solution for the cut networks must satisfy, in order to also be a solution to the original network, and prove that there are parameters that satisfy these constraints.

Before we prove Theorem 3.8, we derive an equivalent characterization of the solvability of the mixture model (2.15). At the end of this section, we appy this characterization to conclude that the mixture model (2.15) admits at least one solution. We start by introducing the notion of a *cut graph* to formalize the process of cutting the edges of a graph.

Definition 3.11 (Cut graph, cf. [28, 29])**.** Let $\mathcal{G}$ be a graph and let $e^c = (f(e^c), h(e^c))$ be an edge of $\mathcal{G}$. Then the so-called *cut graph* $\mathcal{G}^c = (\mathcal{V}^c, \mathcal{E}^c)$ of $\mathcal{G}$ with respect to e^c is defined by

$$\mathcal{V}^c = \mathcal{V} \cup \{v_{\mathrm{cl}}, v_{\mathrm{cr}}\}, \quad \mathcal{E}^c = (\mathcal{E} \setminus \{e^c\}) \cup \{e_{\mathrm{cl}}, e_{\mathrm{cr}}\},$$

where the nodes $v_{\mathrm{cl}}, v_{\mathrm{cr}} \notin \mathcal{V}$ are generated by cutting the edge e^c which splits into the two new edges $e_{\mathrm{cl}} = (f(e^c), v_{\mathrm{cl}})$ and $e_{\mathrm{cr}} = (v_{\mathrm{cr}}, h(e^c))$, see Figure 4 for a visualization.

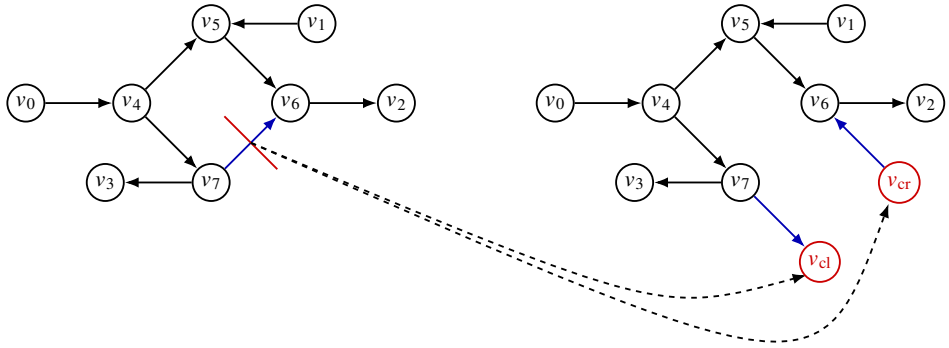

Figure 4. A graph with a single circle (left) and the resulting cut graph when cutting the blue edge (right).

Since our goal is to find solutions to the mixture model on the cut graph $\mathcal{G}^c$ that are also solutions to the original graph $\mathcal{G}$, we assume that the boundary data for all old nodes $v \in \mathcal{V}$ remains the same. At the new nodes $v \in \{v_{\mathrm{cl}}, v_{\mathrm{cr}}\}$, a solution for the cut graph $\mathcal{G}^c$ – indicated by the superscript c – must satisfy three conditions, in order to be a solution for the original graph $\mathcal{G}$ as well:

(c.i) $b^c_{v_{\mathrm{cl}}} = -b^c_{v_{\mathrm{cr}}}$, (c.ii) $\eta^c_{v_{\mathrm{cl}}} = \eta^c_{v_{\mathrm{cr}}}$, (c.iii) $p^c_{v_{\mathrm{cl}}} = p^c_{v_{\mathrm{cr}}}$.

The first condition (c.i) guarantees that the amount of gas leaving the node v_{cl} is equal to the amount of gas entering the node v_{cr}. One can also think of this condition as an invisible pipe connecting the nodes v_{cl} and v_{cr}, ensuring that the gas flow through the cut is constant. The condition (c.ii) and the condition (c.iii) ensure that the composition and the pressure are constant through the cut, respectively.

Next, we introduce appropriate boundary data for the newly introduced nodes v_{cl} and v_{cr} to guarantee that the problem on the cut graph is well-defined and to ensure that the condition (c.i) is always satisfied. Therefore, we introduce the parameter $\lambda \in \mathbb{R}$ and we set

$$b^c_{v_{\mathrm{cl}}} = \lambda \quad \text{and} \quad b^c_{v_{\mathrm{cr}}} = -\lambda.$$

Further, we introduce a second parameter $\mu \in [0,1]$ to model the composition of the supply at the nodes v_{cl} and v_{cr} depending on the sign of λ. Then, the full boundary data for the gas flow model on the cut graph is given by

$$p^c_{v^*} = p^*, \quad b^c_v = \begin{cases} b_v, & v \in \mathcal{V}, \\ -\lambda, & v = v_{\mathrm{cr}}, \\ \lambda, & v = v_{\mathrm{cl}}, \end{cases} \quad \text{and} \quad \zeta^c_v = \begin{cases} \zeta_v, & v \in \mathcal{V}_{<0}, \\ \mu, & v = v_{\mathrm{cr}} \text{ and } \lambda \le 0, \\ \mu, & v = v_{\mathrm{cl}} \text{ and } \lambda > 0. \end{cases}$$

We also have to set the length, diameter, and friction factor of the edges $e \in \{e_{\mathrm{cl}}, e_{\mathrm{cr}}\}$ generated by the cut. We set the edge length to half the length of the cut edge e^c, i.e., we have $L_e = \frac{1}{2} L_{e^c}$ for $e \in \{e_{\mathrm{cl}}, e_{\mathrm{cr}}\}$. Since we assume that all edges have the same diameter and the same friction factor, this property transfers to the two new edges.

We rewrite the condition of constant composition and constant pressure through the cut by using the following functions:

$$H_p \colon \mathbb{R} \times [0,1] \to \mathbb{R}, \quad H_p(\lambda,\mu) = p^c_{v_{\mathrm{cr}}}(\lambda,\mu)^2 - p^c_{v_{\mathrm{cl}}}(\lambda,\mu)^2 \tag{3.4a}$$

$$H_\eta \colon \mathbb{R} \times [0,1] \to \mathbb{R}, \quad H_\eta(\lambda,\mu) = \eta^c_{v_{\mathrm{cr}}}(\lambda,\mu) - \eta^c_{v_{\mathrm{cl}}}(\lambda,\mu), \tag{3.4b}$$

which measure the difference between the pressure and the composition at the new nodes, respectively. Then the task of finding the parameters λ and μ, which satisfy the constraints (c.i)–(c.iii), becomes:

$$\text{Find} \quad (\lambda,\mu) \in \mathbb{R} \times [0,1] \quad \text{such that} \quad H_p(\lambda,\mu) = 0 \quad \text{and} \quad H_\eta(\lambda,\mu) = 0,$$

which means we have to find a common root of H_p and H_η. With this derivation, we obtain an equivalent characterization for the solvability of the steady-state gas flow model (2.15), which we summarize in the following lemma.

Lemma 3.12. *Let $\mathcal{G} = (\mathcal{V}, \mathcal{E})$ be a graph. Then the following holds:*

The gas flow model (2.15) *has a solution.* $\quad \Leftrightarrow \quad$ *The functions H_p and H_η have a common root.*

Proof. Assume that the steady-state gas flow model (2.15) has a solution p_v, q_e, η_v, and let e^c be the cut edge. Then, by the definition of H_p and H_η, these two functions have the following common root:

$$\lambda^* = q_{e^c} \quad \text{and} \quad \mu^* = \begin{cases} \eta_{f(e^c)}, & \text{if } q_{e^c} \ge 0, \\ \eta_{h(e^c)}, & \text{if } q_{e^c} < 0. \end{cases}$$

Now suppose that H_p and H_η have a common root (λ^*, μ^*). We then recover a solution to the gas

flow model (2.15) by setting

$$q_e = \begin{cases} q_e^c(\lambda^*, \mu^*), & e \in \mathcal{E} \setminus \{e^c\}, \\ \lambda^*, & e = e^c, \end{cases} \qquad \eta_v = \eta_v^c(\lambda^*, \mu^*), \quad \pi_v = \pi_v^c(\lambda^*, \mu^*).$$

If $\pi_v \geq 0$ for all $v \in \mathcal{V}$, we obtain a solution for the nodal pressures by setting $p_v = \sqrt{\pi_v}$.

In case the functions H_p and H_η have a common root, the solvability of the mixture model (2.15), i.e., Theorem 3.8, follows immediately from Lemma 3.12. Therefore, our next goal is to show that the functions H_p and H_η have a common root.

Lemma 3.13. *Let $\mathcal{G} = (\mathcal{V}, \mathcal{E})$ be a directed graph with one cycle and let $e^c \in \mathcal{E}$ be an edge within the cycle. Further, let $\mathcal{G}^c$ be the cut graph obtained by cutting the edge e^c. Then a tuple $(\lambda^*, \mu^*) \in \mathbb{R} \times [0, 1]$ exists such that*

$$H_p(\lambda^*, \mu^*) = 0 \quad \textit{and} \quad H_\eta(\lambda^*, \mu^*) = 0,$$

where the functions H_p and H_η are defined in Equation (3.4)*, i.e., these two functions have at least one common root.*

Before proceeding with the proof of Lemma 3.13, we briefly highlight the additional challenges posed by gas mixtures compared with a single gas. In the case of a single gas, the function H_η and the variable μ disappear as the composition of the gas remains constant. The problem reduces to showing that $H_p(\lambda)$ has a (unique) root. This is comparatively straightforward: In [29], the authors prove that H_p is continuous and strictly monotone, which implies the existence of a unique root with the intermediate value theorem.

For gas mixtures, the boundary data includes not only the load but also the supply composition if the node is a supply node. In particular, at the nodes v_{cl} and v_{cr}, the supply composition is switched on or off when λ switches its sign. This discontinuous behavior, along with the need to solve a nonlinear system rather than a single scalar equation, complicates the task of establishing the continuity of H_p for gas mixtures. Furthermore, the variable composition complicates proving strict monotonicity. As a result, we prove only the existence of a solution, not its uniqueness. We discuss the challenges with respect to monotonicity in Section 4.

Our approach to show the existence is to reduce the non-linear system to a scalar problem by solving $H_\eta(\lambda, \mu) = 0$ for $\mu = \mu(\lambda)$. Then, the idea to prove Lemma 3.13 is as follows:

(i) For a fixed λ, we show that the function H_η admits a unique root $\mu_\eta(\lambda)$, which means that $H_\eta(\lambda, \mu_\eta(\lambda)) = 0$ holds.

(ii) We restrict the function H_p to the root curve $\mu_\eta(\lambda)$ resulting in the scalar function $g(\lambda) = H_p(\lambda, \mu_\eta(\lambda))$. We then apply the intermediate value theorem to the function g to show that it admits at least one root, i.e., we have to show that

   (a) the function g is continuous, and

   (b) values λ^- and λ^+ exist such that $g(\lambda^-) \leq 0$ and $g(\lambda^+) \geq 0$.

In Figure 5, we provide an overview of the intermediate results required and group them into two categories corresponding to the two steps of the proof. In the following, we postpone the detailed proof to show the intermediate results first.

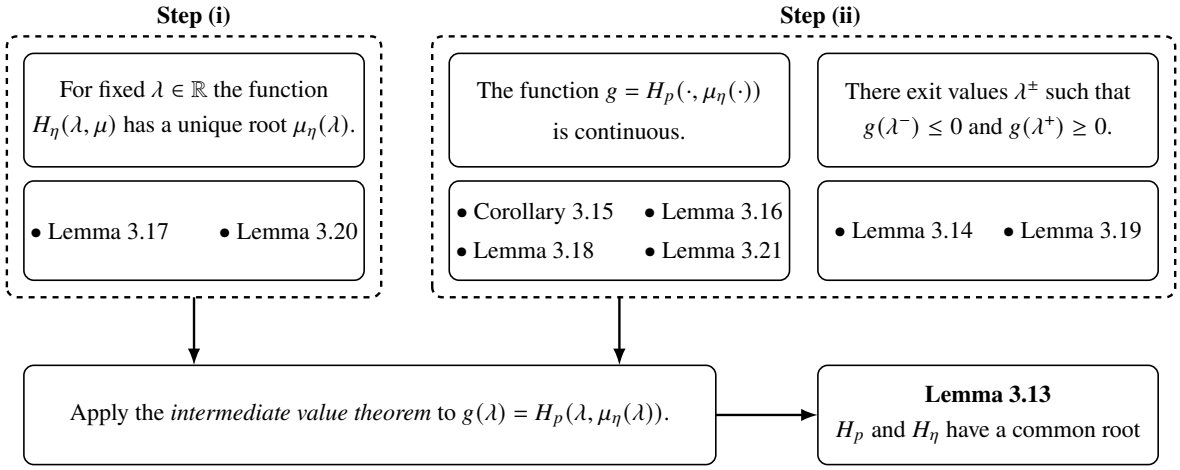

Figure 5. Overview and dependence of the intermediate results to show Lemma 3.13.

To show the two intermediate steps of the proof, we analyze the properties of the nodal composition η_v^c and the flow q_e^c on the edges, because both functions, H_p and H_η, can be written in terms of η_v^c and q_e^c. For the function H_η, this holds by definition. The function H_p describes the pressure change between the node v_{cl} and the node v_{cr}. Hence, we apply Lemma 2.4 to express H_p in terms of η_v^c and q_e^c, which results in

$$H_p(\lambda, \mu) = \sum_{e \in \mathcal{E}_\mathcal{P}} \tilde{\sigma}(\eta^c_{f(e)}(\lambda, \mu), \eta^c_{h(e)}(\lambda, \mu), q_e^c(\lambda)) a^c(v_e, e) q_e^c(\lambda) |a^c(v_e, e) q_e^c(\lambda)|, \tag{3.5}$$

where $\mathcal{E}_\mathcal{P} \subseteq \mathcal{E}^c$ is the set of edges that belong to the path connecting v_{cl} and v_{cr}, and v_e denotes the node of edge e that is closer to the start node of the path.

Thus, besides analyzing the properties of the flow q_e^c and the nodal composition η_v^c, we also show how these properties transfer to the functions H_p and H_η, and how they contribute to the proof of Lemma 3.13.

3.2.1. Properties of the flow and the nodal composition

We start with showing that the flow q_e^c on the edges of the former cycle of the network depends linearly on λ, as this property is essential to ensure that the function H_η admits a unique root, and that the function $\lambda \mapsto H_p(\lambda, \mu_\eta(\lambda))$ satisfies the requirements on the intermediate value theorem.

Lemma 3.14. *Let $\mathcal{G} = (\mathcal{V}, \mathcal{E})$ be a graph with one cycle and let $e^c \in \mathcal{E}$ be the cut edge within the cycle $(C, \mathcal{E}_C)$. Assume that λ and μ are fixed. Then the flow q_e^c on the cut graph $\mathcal{G}^c$ depends linearly on λ and can be written as*

$$a^c(v_e, e) q_e^c(\lambda) = \gamma_e - \lambda \quad \textit{for all} \quad e \in (\mathcal{E}_C \setminus \{e^c\}) \cup \{e_{\mathrm{cl}}, e_{\mathrm{cr}}\},$$

where the constants γ_e depend only on the load b_v, and v_e is the node of the edge e that is closer to the

node v_{cr} (cf., Lemma 2.4 for the definition of v_e).

Proof. Since $\mathcal{G}$ has only one cycle, the cut graph $\mathcal{G}^c$ is tree-shaped. Thus, a unique path connecting v_{cl} and v_{cr} exists, which forms a connected subgraph $(\mathcal{P}, \mathcal{E}_{\mathcal{P}})$ of $\mathcal{G}^c$ with

$$\mathcal{P} = C \cup \{v_{\mathrm{cl}}, v_{\mathrm{cr}}\} \quad \text{and} \quad \mathcal{E}_{\mathcal{P}} = \mathcal{E}_C \setminus \{e^c\} \cup \{e_{\mathrm{cl}}, e_{\mathrm{cr}}\}. \tag{3.6}$$

Without loss of generality, we assume that the path starts at v_{cr} and ends at v_{cl}. Analogous to the proof of [29, Theorem 1], each edge $e \notin \mathcal{E}_{\mathcal{P}}$ is part of a sub-tree of $\mathcal{G}^c$ with one node in $\mathcal{P}$. As the loads b_v^c are fixed and independent of λ for $v \notin \{v_{\mathrm{cl}}, v_{\mathrm{cr}}\}$, the flow q_e^c on these edges is uniquely determined and independent of λ.

For the edges $e \in \mathcal{E}_{\mathcal{P}}$, the mass conservation Eq (2.15b) yields the linear system $A^{\mathcal{P}} \boldsymbol{q}^{\mathcal{P}} = \boldsymbol{b}^{\mathcal{P}}$, where $A^{\mathcal{P}}$ is the incidence matrix of the subgraph of the path, $\boldsymbol{q}^{\mathcal{P}}$ is the flow vector, and $\boldsymbol{b}^{\mathcal{P}}$ isthe vector of adjusted loads. Since $A^{\mathcal{P}}$ is lower triangular, we apply forward substitution to solve the linear system, cf. [29, Theorem 1]:

$$a^c(v_i, e_i) q_{e_i}^c = \sum_{k=1}^{i} b_{v_k}^{\mathcal{P}} \quad \text{with} \quad b_v^{\mathcal{P}} \coloneqq b_v^c - \sum_{e \in \mathcal{E}(v) \setminus \mathcal{E}_{\mathcal{P}}} a^c(v, e) q_e^c \quad \text{for} \quad v \in \mathcal{P}.$$

The numbering of the nodes indicates the order in which they are traversed by the path, i.e., $v_1 = v_{\mathrm{cr}}$ and $v_p = v_{\mathrm{cl}}$ with $p = |\mathcal{P}|$. An edge e_i connects the nodes v_i and v_{i+1}. As the path starts at node $v_1 = v_{\mathrm{cr}}$, we have $a^c(v_1, e_1) q_{e_1}^c = b_{v_1}^{\mathcal{P}} = -\lambda$. Further, the redefined loads $b_v^{\mathcal{P}}$ are independent of λ for $v \notin \{v_1 = v_{\mathrm{cl}}, v_p = v_{\mathrm{cr}}\}$, which leads to

$$a^c(v_i, e_i) q_{e_i}^c = -\lambda + \underbrace{\sum_{k=2}^{i} \left[b_{v_k} - \sum_{e \in \mathcal{E}(v_k) \setminus \mathcal{E}_{\mathcal{P}}} a(v_k, e) q_e^c \right]}_{=: \gamma_{e_i} \text{ which is independent of } \lambda} \quad \text{for} \quad i = 1, \dots p-1$$

$$\Leftrightarrow \quad a^c(v_e, e) q_e^c = \gamma_e - \lambda \quad \text{for} \quad e \in \mathcal{E}_{\mathcal{P}} = (\mathcal{E}_C \setminus \{e^c\}) \cup \{e_{\mathrm{cl}}, e_{\mathrm{cr}}\}.$$

Given this representation of q_e^c on the edges of the former cycle, along with the fact that the flow is independent of λ on all the remaining edges, the continuity of the flow in λ follows immediately.

Corollary 3.15 (Continuity of the flow)**.** *Let the requirements of Lemma 3.14 be satisfied. Then the flow q_e^c on the cut graph $\mathcal{G}^c$ is continuous in λ for all edges $e \in \mathcal{E}^c$.*

Proof. The claim follows directly from the proof of Lemma 3.14 as q_e^c is independent of λ if $e \notin \mathcal{E}_C \cup \{e_{\mathrm{cl}}, e_{\mathrm{cr}}\}$ and linear in λ if $e \in \mathcal{E}_C \cup \{e_{\mathrm{cl}}, e_{\mathrm{cr}}\}$.

The continuity of q_e^c with respect to λ enables us to establish the continuity of the nodal compositions η_v^c. However, the interpretation of the nodes v_{cl} and v_{cr} as the supply or demand nodes depends on the sign of λ: for $\lambda > 0$, v_{cl} is a demand node and v_{cr} is a supply node, while for $\lambda < 0$, their roles are reversed. This sign change can be likened to a supply station that suddenly becomes a consumer, which implies a discontinuity in composition at $\lambda = 0$.

Lemma 3.16 (Continuity of the composition with respect to λ)**.** *Let $\mathcal{G}$ be a graph with a single cycle, $e^c \in \mathcal{E}$ be an edge belonging to the cycle, and $\mathcal{G}^c$ is the resulting cut graph. Assume that $\mu \in [0,1]$ is arbitrary, yet fixed. Then*

(i) The nodal compositions η_v^c are continuous for $\lambda \in \mathbb{R} \setminus \{0\}$.

(ii) The nodal compositions η_v^c are also continuous in $\lambda = 0$ for the nodes $v \in \mathcal{V} \setminus \{v_{\mathrm{cl}}, v_{\mathrm{cr}}\}$.

Proof. We prove the claim by using the concept of a topological ordering to traverse through the nodes of $\mathcal{G}^c$. The graph $\mathcal{G}^c_{\mathrm{flow}}$ has the same nodes as the cut graph $\mathcal{G}^c$ but its edges align with the flow direction. Further, the graph $\mathcal{G}^c_{\mathrm{flow}}$ is tree-structured and thus has a topological order of its nodes.

The flow along the path between the nodes v_{cl} and v_{cr} only changes when λ changes because the cut graph $\mathcal{G}^c$ is tree-shaped. Lemma 3.14 allows us to determine flow direction of an edge belonging to this path depending on λ, as well as at which value of λ the flow of an edge becomes zero. We sort these roots in ascending order as follows:

$$\gamma_{\min} = \tilde{\gamma}_1 < \cdots < \tilde{\gamma}_{|\mathcal{E}_{\mathcal{P}}|} = \gamma_{\max} \quad \text{where} \quad \{\gamma_e \mid e \in \mathcal{E}_{\mathcal{P}}\} = \{\tilde{\gamma}_i \mid i = 1, \dots, |\mathcal{E}_{\mathcal{P}}|\}.$$

Then, for a fixed i, the flow directions are the same for all $\lambda \in (\tilde{\gamma}_i, \tilde{\gamma}_{i+1})$. Thus, the topological ordering differs for each subinterval $(\tilde{\gamma}_i, \tilde{\gamma}_{i+1})$ as the flow directions depend on λ. Now, we show the continuity of η_v^c with respect to λ on $(\tilde{\gamma}_i, \tilde{\gamma}_{i+1})$ by induction over the position k in the topological ordering for a fixed yet arbitrary index $i \in \{1, \dots, |\mathcal{E}_{\mathcal{P}}|\}$.

The first node v in the ordering has to be a supply node where the composition is given through the boundary data, i.e., $\eta_v^c = \zeta_v^c$ is constant and hence is continuous in λ.

In the induction step, we assume that all compositions up to position k are continuous on the subinterval and that v is the node at position $k+1$. Then the composition η_v^c is given by

$$\eta_v^c = \frac{\sum_{e \in \mathcal{E}(v)} \eta_{w_e}^c \left(a^c(v,e) q_e^c\right)^+ + \zeta_v^c (b_v^c)^-}{\sum_{e \in \mathcal{E}(v)} \left(a^c(v,e) q_e^c\right)^+ + (b_v^c)^-} \quad \text{where} \quad w_e = \begin{cases} f(e), & \text{if } v = h(e), \\ h(e), & \text{if } v = f(e). \end{cases}$$

Because the topological ordering is based on the graph with edges in the flow direction, the inflow comes from nodes previous in the ordering. Thus, by the induction assumption, we know that the compositions $\eta_{w_e}^c$ and the flows q_e^c are continuous on the subinterval, and since $a^c(v,e) q_e^c \neq 0$ by definition of the subinterval, we also never divide by zero. Hence, the compositions η_v^c are continuous for $\lambda \neq \tilde{\gamma}_i$. The continuity for the intervals $(-\infty, \tilde{\gamma}_0)$ and $(\tilde{\gamma}_{|\mathcal{E}_{\mathcal{P}}|}, \infty)$ follows analogously.

It remains to prove the continuity in $\lambda = \tilde{\gamma}_i$. Let $\tilde{e} \in \mathcal{E}$ be an edge with $q_{\tilde{e}}(\tilde{\gamma}_i) = 0$. Then, the continuity of η_v^c in $\lambda = \tilde{\gamma}_i$ follows directly for nodes v that are not incident to e. For nodes that are incident to $\tilde{e}$, two cases occur, as follows:

(i) $a^c(v,\tilde{e}) q_{\tilde{e}}^c < 0$ for $\lambda < \tilde{\gamma}_i \quad \Rightarrow \quad a^c(v,\tilde{e}) q_{\tilde{e}}^c > 0$ for $\lambda > \tilde{\gamma}_i$, and

(ii) $a^c(v,\tilde{e}) q_{\tilde{e}}^c > 0$ for $\lambda < \tilde{\gamma}_i \quad \Rightarrow \quad a^c(v,\tilde{e}) q_{\tilde{e}}^c < 0$ for $\lambda > \tilde{\gamma}_i$.

We first demonstrate how to handle case (i). Let v be a node that is incident to $\tilde{e}$; then the following holds:

$$\lim_{\lambda \to \tilde{\gamma}_i -} \eta_v^c(\lambda, \mu) = \lim_{\lambda \to \tilde{\gamma}_i -} \frac{\sum_{e \in \mathcal{E}(v) \setminus \{\tilde{e}\}} \eta_{w_e}^c \left(a^c(v,e) q_e^c\right)^+ + \zeta_v^c (b_v^c)^-}{\sum_{e \in \mathcal{E}(v) \setminus \{\tilde{e}\}} \left(a^c(v,e) q_e^c\right)^+ (b_v^c)^-}$$

$$= \frac{\sum_{e\in\mathcal{E}(v)\setminus\{\tilde{e}\}} \eta^c_{w_e} \left(a^c(v,e)q^c_e\right)^+ + \zeta^c_v (b^c_v)^-}{\sum_{e\in\mathcal{E}(v)\setminus\{\tilde{e}\}} (a^c(v,e)q^c_e)^+ + (b^c_v)^-}$$
$$= \lim_{\lambda\to\tilde{\gamma}_i+} \frac{\sum_{e\in\mathcal{E}(v)} \eta^c_{w_e} \left(a^c(v,e)q^c_e\right)^+ + \zeta^c_v (b^c_v)^-}{\sum_{e\in\mathcal{E}(v)} (a^c(v,e)q^c_e)^+ + (b^c_v)^-} = \lim_{\lambda\to\tilde{\gamma}_i+} \eta^c_v(\lambda,\mu),$$

which proves the continuity of η^c_v for $v \in \mathcal{V}\setminus\{v_{\mathrm{cl}}, v_{\mathrm{cr}}\}$. Notice, that the nodes v_{cr} and v_{cl} lead to a special case, since both nodes are boundary nodes and their load b^c_v can change depending on the value of λ. In particular, both nodes can switch between being the supply and demand node when λ switches its sign. Hence, the compositions η^c_v are discontinuous in $\lambda = 0$ in general for $v \in \{v_{\mathrm{cl}}, v_{\mathrm{cr}}\}$. Case (ii) is analogous to case (i).

The continuity of the composition with respect to μ follows from the fact that each nodal composition η_v is either independent of μ or depends linearly on it.

Lemma 3.17 (Continuity of the composition with respect to μ)**.** *Let $\mathcal{G}$ be a graph with a single cycle, $e^c \in \mathcal{E}$ be an edge belonging to the cycle, and $\mathcal{G}^c$ be the resulting cut graph. Moreover, let $u \in \mathcal{V}^c_{<0}$ be a supply node with the supply composition ζ^c_u and let q^c_e be a flow on the network satisfying Eq (2.15b). Then for every node $v \in \mathcal{V}^c$, one of the following two cases apply:*

(i) The nodal composition η^c_v depends linearly on ζ^c_u.

(ii) The nodal composition η^c_v is independent of ζ^c_u.

Further, the nodal compositions are well-defined, meaning that $\eta^c_v \in [0,1]$ for all $v \in \mathcal{V}^c$, if the boundary data satisfy $\zeta^c_v \in [0,1]$ for every supply node $v \in \mathcal{V}^c_{<0}$.

Proof. A topological ordering of the nodes of $\mathcal{G}^c_{\mathrm{flow}}$ exists since we cut the only cycle of $\mathcal{G}$ and we can prove the claim by induction over the position k in the ordering.

The node at position $k = 1$ must be a supply node where $b^c_v < 0$ holds. Therefore, η^c_v is given directly by the boundary data, which implies that η_v is independent of ζ^c_u if $v \neq u$ and is linear in ζ^c_u if $v = u$. By choice of the boundary data, we have $\eta^c_v \in [0,1]$.

Now, assume that the claim holds for all nodes up to position k in the ordering. Let v be the node at position $k+1$. Then two cases can apply: (a) v is a supply node, or (b) v is not. Case (a) is analogous to the case $k = 1$. In Case (b), the composition can be computed by

$$\eta^c_v = \frac{\sum_{e\in\mathcal{E}(v)} \eta^c_{w_e} \left(a^c(v,e)q^c_e\right)^+ + \zeta^c_v (b^c_v)^-}{\sum_{e\in\mathcal{E}(v)} (a^c(v,e)q^c_e)^+ + (b^c_v)^-} \quad \text{where} \quad w_e = \begin{cases} f(e), & \text{if } v = h(e), \\ h(e), & \text{if } v = f(e). \end{cases}$$

As the gas flows from nodes early in the ordering to nodes later in the ordering, we know, by the induction assumption, that the compositions $\eta^c_{w_e}$ are linear or independent of ζ^c_w and $\eta^c_{w_e} \in [0,1]$.

3.2.2. Properties of the functions H_p and H_η

The next step is to extend the results for the flow q^c_e and composition η^c_v to the functions H_p and H_η, since both functions depend on these variables, cf., Eqs (3.4) and (3.5). First, we show that the function H_p is continuous in λ and μ as the flow and the composition are continuous too.

Lemma 3.18 (Properties of H_p)**.** *The function $H_p\colon \mathbb{R}\times[0,1]\to\mathbb{R}$ is*

(i) linear in μ and hence, continuous and monotone in μ,

(ii) continuous in λ, and

(iii) constant in μ if $\lambda = 0$.

Proof. The function H_p describes the pressure change along the path connecting the nodes v_{cl} and v_{cr}. Hence, we apply Lemma 2.4 to obtain an alternative expression of H_p as follows:

$$H_p(\lambda,\mu) = \sum_{e\in\mathcal{E}_\mathcal{P}} \tilde{\sigma}(\eta^c_{f(e)}(\lambda,\mu), \eta^c_{h(e)}(\lambda,\mu), q^c_e(\lambda))a^c(v_e,e)q^c_e(\lambda)|a^c(v_e,e)q^c_e(\lambda)|,$$

where v_e is the node of the edge e that is closer to node v_{cl}. Since the cut graph $\mathcal{G}^c$ is tree-shaped, the flow q^c_e is fully determined by the loads b^c_v. Thus, the flow q^c_e along the edges only depends on the parameter λ but not on the parameter μ.

(i) The linearity of H_p with respect to μ follows directly from the linearity of the composition η_v with respect to μ; cf., Lemma 3.17.

(ii) The argument to show the continuity with respect to λ is similar. The continuity in $\lambda \neq 0$ follows from the continuity of the flow (Corollary 3.15) and the continuity of the composition (Lemma 3.16). In order to also prove the continuity in $\lambda = 0$, we rewrite the function H_p as

$$H_p(\lambda,\mu) = \underbrace{\sum_{\substack{e\in\mathcal{E}_\mathcal{P}\\ e\neq e_{\mathrm{cl}},e_{\mathrm{cr}}}} \tilde{\sigma}(\eta^c_{f(e)}(\lambda,\mu), \eta^c_{h(e)}(\lambda,\mu), q^c_e(\lambda))a^c(v_e,e)q^c_e(\lambda)|a^c(v_e,e)q^c_e(\lambda)|}_{\text{continuous in } \lambda=0 \text{ by Corollary 3.15 and Lemma 3.16}}$$
$$+ \underbrace{\tilde{\sigma}(\eta^c_{v_{\mathrm{cr}}}(\lambda), \eta^c_{h(e_{\mathrm{cr}})}(\lambda,\mu),\lambda)\lambda|\lambda| + \tilde{\sigma}(\eta^c_{f(e_{\mathrm{cl}})}(\lambda,\mu), \eta^c_{v_{\mathrm{cl}}}(\lambda),\lambda)\lambda|\lambda|}_{\eta^c_{v_{\mathrm{cl}}} \text{ and } \eta^c_{v_{\mathrm{cr}}} \text{ are in general discontinuous in } \lambda=0}.$$

Although the compositions $\eta^c_{v_{\mathrm{cl}}}$ and $\eta^c_{v_{\mathrm{cr}}}$ are discontinuous at $\lambda = 0$ by Lemma 3.16, the function H_p is continuous at $\lambda = 0$ because terms of the form $\tilde{\sigma}(\eta^c_{f(e)}, \eta^c_{h(e)}, \lambda)\lambda|\lambda|$ are continuous at $\lambda = 0$ even if the compositions $\eta^c_{f(e)}$ and $\eta^c_{h(e)}$ are not. This is because the function $\tilde{\sigma}$ is bounded from above, which leads to

$$\left|\tilde{\sigma}(\eta^c_{f(e)}, \eta^c_{h(e)}, \lambda)\lambda|\lambda|\right| \leq \frac{\lambda_{\mathrm{Fr}} L_e}{D} \max\{\sigma^2_{\mathrm{H_2}}, \sigma^2_{\mathrm{NG}}\}\lambda^2 \longrightarrow 0 \quad \text{for} \quad \lambda \longrightarrow 0.$$

Hence, the discontinuity vanishes for $\lambda = 0$ and H_p is continuous at every λ.

(iii) Finally, we prove that H_p is constant in μ if $\lambda = 0$. As the flow is fully determined by the loads, the dependence on the parameter μ is given by the mixing equation, specifically, through the term $\mu\lambda^2$ when computing the nodal composition η^c_v. Hence, if $\lambda = 0$, the nodal compositions are independent of μ and we get $H_p(0,\mu) \equiv \text{const}$.

Next, we identify for which values of λ the flow is either directed from node v_{cl} to node v_{cr} or vice versa. As the function H_p describes the pressure change along the path connecting v_{cl} and v_{cr}, this allows us to determine the sign of H_p for these values of λ.

Lemma 3.19 (Unidirectional flow)**.** *Assume that the requirements of Lemma 3.14 are satisfied and define* $\gamma_{\min} = \min_{e\in C\setminus\{e^c\}} \gamma_e$ *and* $\gamma_{\max} = \max_{e\in C\setminus\{e^c\}} \gamma_e$*. Then:*

(i) The gas flows from v_{cr} *to* v_{cl} *if and only if* $\lambda \geq \gamma_{\max}$*, which implies* $H_p(\lambda, \mu) \geq 0$*.*

(ii) The gas flows from v_{cl} *to* v_{cr} *if and only if* $\lambda \leq \gamma_{\min}$*, which implies* $H_p(\lambda, \mu) \leq 0$*.*

Proof. Since the requirements of Lemma 3.14 are satisfied, the cut graph $\mathcal{G}^c$ is tree-shaped and thus there is only one path connecting the nodes v_{cl} and v_{cr}. Consider the subgraph of $\mathcal{G}^c$ that forms the path between v_{cr} and v_{cl}, which we denote by

$$(\mathcal{P}, \mathcal{E}_{\mathcal{P}}) \quad \text{where} \quad \mathcal{P} = C \cup \{v_{\mathrm{cl}}, v_{\mathrm{cr}}\} \quad \text{and} \quad \mathcal{E}_{\mathcal{P}} = (\mathcal{E}_C \setminus \{e^c\}) \cup \{e_{\mathrm{cl}}, e_{\mathrm{cr}}\}.$$

We assume, without loss of generality, that the path starts at v_{cr} and ends at v_{cl}. Then the flow directed from v_{cr} to v_{cl} translates into $a^c(v_e, e)q_e^c \leq 0$ and the flow with the opposite direction translates into $a^c(v_e, e)q_e^c \geq 0$ for all $e \in \mathcal{E}_{\mathcal{P}}$. Consider the first case. Then, by Lemma 3.14, we get

$$a^c(v_e, e)q_e^c = \gamma_e - \lambda \leq \gamma_e - \gamma_{\max} \leq 0 \quad \text{for all } e \in \mathcal{E}_{\mathcal{P}} \quad \Leftrightarrow \quad \lambda \geq \lambda_{\max},$$

which means that the gas flows from node v_{cr} to node v_{cl}. The node v_e is the node of the edge e which is closer to node v_{cr}. We now apply Lemma 2.4, which yields

$$H_p(\lambda, \mu) = p^c_{v_{\mathrm{cr}}}(\lambda, \mu)^2 - p^c_{v_{\mathrm{cl}}}(\lambda, \mu)^2 \geq 0.$$

The second case follows analogously.

From Lemma 3.17, we know that the composition η_v^c depends linearly on μ. As the function H_η is the difference between two nodal compositions, it is clear that it also depends linearly on μ. We exploit this linearity in the next lemma to prove that H_η has a unique root.

Lemma 3.20 (Root curves of H_η)**.** *The function* $H_\eta \colon \mathbb{R} \times [0, 1]$ *with*

$$H_\eta(\lambda, \mu) = \eta^c_{v_{\mathrm{cr}}}(\lambda, \mu) - \eta^c_{v_{\mathrm{cl}}}(\lambda, \mu),$$

is linear in μ*. Furthermore, for a fixed* λ*, the function* H_η *admits a unique root* $\mu_\eta(\lambda)$*. For* $\lambda \in [\gamma_{\min}, \gamma_{\max}]$ *the root is given by:*

$$\mu_\eta(\lambda) = \begin{cases} \eta^c_{v_{\mathrm{cr}}}(\lambda), & \lambda < 0, \\ \eta^c_{v_{\mathrm{cl}}}(\lambda), & \lambda \geq 0. \end{cases}$$

Proof. The linearity of H_η for a fixed λ follows immediately from Lemma 3.17. Due to the linearity, it is also clear that $H_\eta(\lambda, \mu) = 0$ has a unique solution for a fixed λ. The goal now is to determine the explicit solution to this equation for $\lambda \in [\gamma_{\min}, \gamma_{\max}]$. We distinguish among four cases:

(i) $\lambda = \gamma_{\min}$, (ii) $\lambda \in (\gamma_{\min}, 0)$, (iii) $\lambda \in [0, \gamma_{\max})$, (iv) $\lambda = \gamma_{\max}$.

First, we consider the case of $\lambda \in [0, \gamma_{\max})$. In this case, we know that v_{cr} is a supply node with the composition $\eta^c_{v_{\mathrm{cr}}} = \mu$ and that v_{cl} is a demand node with the composition $\eta^c_{v_{\mathrm{cl}}}(\lambda, \mu)$ due to the sign of λ. Then, the composition $\eta^c_{v_{\mathrm{cl}}}$ is independent of μ.

Considering the opposite, the flow along the path connecting v_{cr} and v_{cl} must be directed from v_{cr} to v_{cl}, which contradicts the assumption $\lambda \leq \gamma_{\max}$ due to Lemma 3.19. Thus, we determine the root of H_η for a fixed λ as follows:

$$H_\eta(\lambda, \mu) = 0 \quad \Leftrightarrow \quad \mu - \eta^c_{v_{\mathrm{cl}}}(\lambda) = 0 \quad \Leftrightarrow \quad \mu_\eta(\lambda) = \eta^c_{v_{\mathrm{cl}}}(\lambda).$$

The case $\lambda \in (\gamma_{\min}, 0)$ follows analogously.

Next, we consider the case $\lambda = \gamma_{\max}$. Then the flow of at least one of the edges of the path connecting v_{cr} and v_{cl} is zero. Furthermore, $a(v_e, e)q^c_e \leq 0$ holds for all edges e of the path. In this scenario, no flow from node v_{cr} can reach node v_{cl}, since at least one edge along the path has a flow of zero, even though technically the flow is directed from v_{cr} to v_{cl}. Thus, the composition $\eta^c_{v_{\mathrm{cl}}}$ is again independent of μ and we can compute the root as for the case where $\lambda \in [0, \gamma_{\max})$. Again, the case $\lambda = \gamma_{\min}$ follows analogously.

The structure of the root curve μ_η of H_η for $\lambda \in [\gamma_{\min}, \gamma_{\max}]$ allows us to directly show its continuity, since the root curve is given by the nodal composition either of the node v_{cl} or of the node v_{cr}, depending on the sign of λ.

Lemma 3.21 (Continuity of the root curve μ_η)**.** *The root curve $\mu_\eta\colon [\gamma_{\min}, \gamma_{\max}] \to [0, 1]$ defined in Lemma 3.20 is continuous in $\lambda \in [\gamma_{\min}, \gamma_{\max}] \setminus 0$.*

Proof. The claim follows directly from Lemma 3.16.

Finally, we are equipped to prove that the two functions H_p and H_η have a common root (Lemma 3.13). We recall the structure of the idea of the proof and indicate where the results from Sections 3.2.1 and 3.2.2 come into play.

(i) For a fixed λ, Lemma 3.20 shows that the function H_η has a unique root $\mu_\eta(\lambda)$.

(ii) We then restrict the function H_p to the root curve $\mu_\eta(\lambda)$ and apply the intermediate value theorem to the restricted function $g(\lambda) = H_p(\lambda, \mu_\eta(\lambda))$, which requires the following

  (a) the function g is continuous (Lemmas 3.18 and 3.21), and

  (b) the values λ^- and λ^+ exist such that $g(\lambda^-) \leq 0$ and $g(\lambda^+) \geq 0$ (Lemma 3.19).

In the following, we provide the detailed proof of Lemma 3.13.

Proof of Lemma 3.13. We distinguish between two cases: The case where $\lambda = 0$ lies in the interior of $[\gamma_{\min}, \gamma_{\max}]$, and the case where $\lambda = 0$ lies on the boundary of the interval.

First, we consider the case where $\lambda = 0$ lies in the interior of $[\gamma_{\min}, \gamma_{\max}]$. From Lemma 3.20, it follows that the equation $H_\eta(\lambda, \mu_\eta(\lambda)) = 0$ has a unique solution $\mu_\eta(\lambda)$ for a fixed $\lambda \in [\gamma_{\min}, \gamma_{\max}]$. The idea of the proof is now to use the root curve μ_η to define an auxiliary function

$$g\colon [\gamma_{\min}, \gamma_{\max}] \to \mathbb{R}, \quad g(\lambda) = H_p(\lambda, \mu_\eta(\lambda)),$$

and show that g has at least one root in $[\gamma_{\min}, \gamma_{\max}]$ by applying the intermediate value theorem. Once we have a root λ^* of g, we set $\mu^* = \mu_\eta(\lambda^*)$. The remaining part is to verify the requirements of the intermediate value theorem.

(a) g is continuous on $[\gamma_{\min}, \gamma_{\max}]$, (b) $g(\gamma_{\min}) \leq 0$ and $g(\gamma_{\max}) \geq 0$.

We start by proving the continuity of g. From Lemma 3.21, it follows that the root curve μ_η is continuous on $[\gamma_{\min}, \gamma_{\max}] \setminus \{0\}$. Furthermore, we know that H_p is continuous (Lemma 3.18), which immediately provides the continuity of g for $\lambda \neq 0$. Thus, it remains to show the continuity of g in $\lambda = 0$. Recall that from Lemma 3.18, it also follows that $H_p(0, \cdot)$ is constant, i.e., $\alpha \in \mathbb{R}$ exists such that $H_p(0, \mu) = \alpha$ for all $\mu \in [0, 1]$ which leads to:

$$\lim_{\lambda \to 0-} g(\lambda) = \lim_{\lambda \to 0-} H_p(\lambda, \mu_\eta(\lambda)) = H_p(0, \lim_{\lambda \to 0-} \mu_\eta(\lambda)) = \alpha$$
$$\alpha = H_p(0, \lim_{\lambda \to 0+} \mu_\eta(\lambda)) = \lim_{\lambda \to 0+} H_p(\lambda, \mu_\eta(\lambda)) = \lim_{\lambda \to 0+} g(\lambda).$$

After we have established the continuity of g, Requirement (b) follows immediately from Lemma 3.19, which completes the proof for this case.

Next, we consider the case where $\lambda = 0$ lies on the boundary of $[\gamma_{\min}, \gamma_{\max}]$. Then either $\gamma_{\min} = 0$ or $\gamma_{\max} = 0$. Let us assume that $\gamma_{\min} = 0$, as the other case follows analogously. Since H_p is continuous on $[\gamma_{\min}, \gamma_{\max}]$ and constant in $\lambda = 0$, an $\varepsilon > 0$ independent of μ exists such that

$$\operatorname{sign}(H_p(0, \mu)) = \operatorname{sign}(H_p(\varepsilon, \mu)).$$

Hence, we can apply the same argument to the interval $[\varepsilon, \gamma_{\max}]$ as that for the case where $\lambda = 0$ lies in the interior of the interval $[\gamma_{\min}, \gamma_{\max}]$.

After we have proved Lemma 3.13, we automatically find that the mixture model (2.15) has at least one solution, which proves our main result, Theorem 3.8.

Proof of Theorem 3.8. Due to Lemma 3.12, the solvability of the mixture model (2.15) is equivalent to the functions H_p and H_η having at least one common root, which follows from Lemma 3.13 and thus proves the claim.

Remark 3.22. So far, we have considered (passive) networks with at most one cycle, but the argumentation can also be applied to networks with active elements such as compressors, as long as they are not parallel to the edges or within cycles. Furthermore, the compressor ratio must be independent of the composition and flow.

For tree-shaped networks, the flows q_e and the compositions η_v are uniquely determined by the conservation of mass and the mixing at the nodes, regardless of whether the network contains active elements or not. Thus, a solution for the nodal potentials π_v exists and it is also unique for networks with compressors. To prove the existence of a solution for single-cycle networks, we use the function H_p. For networks with one cycle and compressors outside of the cycle, the structure of H_p is the same as in Eq (3.5). Therefore, proving the existence of solutions is identical to proving Theorem 3.8. If the compressors are inside the cycle, the compressor ratios enter the function H_p, i.e., some summands are multiplied by the compressor ratios. Which summands are affected depends on the position of the

compressors in the cut cycle. As the compressor ratios are constant, again, the idea of the proof of Theorem 3.8 still applies.

4. Discussion on uniqueness and multiple cycles

After establishing the existence of steady states, we discuss theoretical limitations in this section. On the one hand, we present an idea of how the proof can be extended to networks with multiple cycles, while also highlighting the difficulties that arise compared with networks with one cycle. On the other hand, we address the question of unique solutions and emphasize the challenges in proving uniqueness for systems involving gas mixtures compared with a single gas.

4.1. Existence of solutions for networks with multiple cycles

So far, we have restricted our theoretical investigation to networks with at most one cycle, and we did not consider networks with multiple cycles. To prove the existence of nodal potentials for networks with multiple cycles, we employ an induction argument on the number of cycles in the network. In Section 3.2, we have presented the first induction step, going from networks without cycles to networks with one cycle. However, networks with multiple cycles pose new challenges when performing induction, since the cut graph of such networks is no longer tree-shaped.

One consequence is that the flow q_e^c on the edges of the cut graph is not fully determined by the loads b_v^c, i.e., it also depends on the supply composition ζ_v^c and the fixed pressure p^*. As the flow q_e^c now depends on both parameters λ and μ, the composition η_v^c at a node v becomes non-linear in μ. The function H_η inherits the non-linearity and it becomes unclear whether the equation $H_\eta(\lambda, \mu) = 0$ admits a (unique) solution for every $\lambda \in \mathbb{R}$.

We illustrate this non-linearity in Figure 6 for the network shown in Figure 4 but with an additional edge connecting the nodes v_5 and v_7, i.e., the cut edge. The boundary data are given in Table 1. In Figure 6, we plot the composition $\eta_{v_4}^c$ as a function of μ for different values of λ, clearly showing the nonlinear dependence on μ. Thus, the analysis of the non-linearity and its influence on the solvability of $H_\eta(\lambda, \mu) = 0$ remains as a subject for future research.

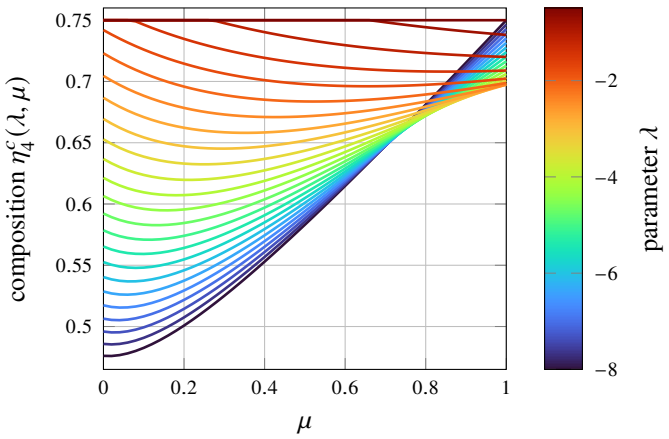

Figure 6. The nodal composition $\eta_{v_4}^c(\lambda, \mu)$ as a function of μ for different values of λ. The value of λ is encoded by the color bar.

Table 1. Boundary data at the nodes.

Supply		Demand	Pressure
Composition	Load		
$\zeta_{v_0} = \frac{3}{4}$	$b_{v_0} = 4$	$b_{v_2} = -2$	$p_{v_0} = p^* = 60$
$\zeta_{v_1} = \frac{1}{4}$	$b_{v_1} = 4$	$b_{v_3} = -6$	

Despite the non-linearity, we can still solve the mixture model (2.15) numerically, e.g., with the Levenberg–Marquardt method, which allows us to compute the functions H_p and H_η for a fixed example and analyze their properties. On the basis of the same network configuration and boundary conditions as for Figure 6, we display both functions H_p and H_η in Figure 7.

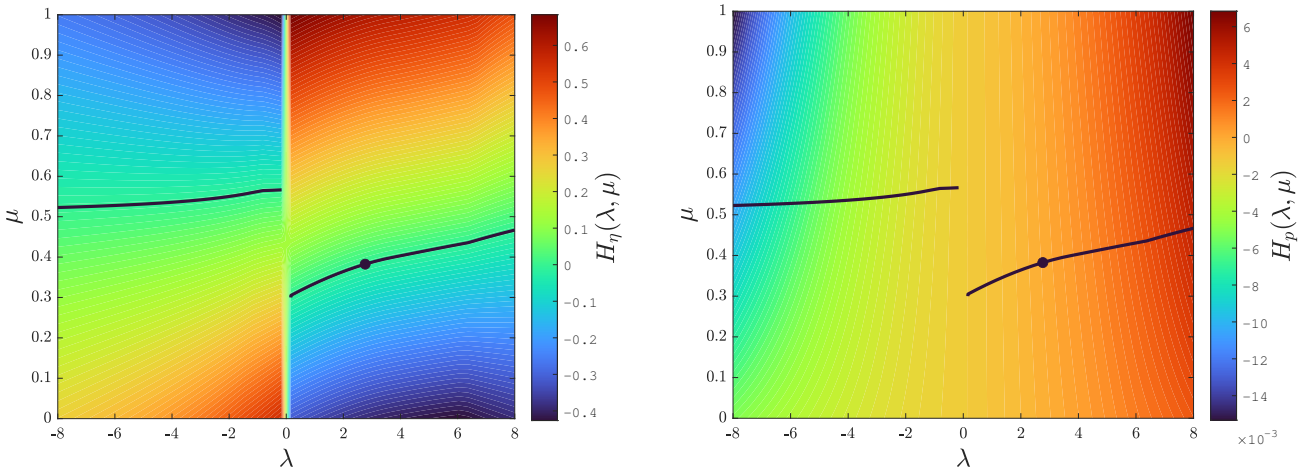

Figure 7. The functions $H_\eta(\lambda, \mu)$ (left) and $H_p(\lambda, \mu)$ (right) for a network with two cycles. The black dot is the common root (λ^*, μ^*), and the black line the root curve $\mu_\eta(\lambda)$.

Consistent with the behavior described in Lemma 3.16, we observe that the function H_η is discontinuous at $\lambda = 0$ for all $\mu \in [0, 1]$. Furthermore, in analogy to Lemma 3.19, the function H_p has opposite signs for $\lambda = -8$ and $\lambda = 8$. Figure 7, also shows the root curve μ_η of the function H_η, defined as the level set $H_\eta(\lambda, \mu) = 0$, which indicates that $H_\eta(\lambda, \mu) = 0$ has a unique solution for a fixed λ, cf., Lemma 3.20. We also observe that the root curve μ_η is discontinuous at $\lambda = 0$, which is analogous to Lemma 3.21 for networks with one cycle. Python's "get_path()" function for contour plots allows us to extract the coordinates of a level set. Thus, we can evaluate H_p along the root curve μ_η, which results in the scalar function $g(\lambda) = H_p(\lambda, \mu_\eta(\lambda))$. Then Figure 8(b) reveals that the function g is continuous in $\lambda = 0$ despite the discontinuity of the root curve μ_η. Furthermore, we observe that g increases strictly monotonically with a unique root λ^*, implying that the solution of the mixture model (2.15) is unique, cf. Lemma 3.12.

In summary, numerical experiments suggest that the idea of the proof of Theorem 3.8 also applies to networks with multiple cycles. However, to successfully extend the proof, we need to prove rigorously that $H_\eta(\lambda, \mu) = 0$ admits a unique solution for these types of networks, which remains an open question.

4.2. Uniqueness of steady states

We have established unique steady states for gas mixtures only for tree-shaped networks, cf., Theorem 3.5. In contrast, for single gas flow, the uniqueness holds even for general networks, as shown in [29, Theorem 1], raising the question whether this can be extended to gas mixtures.

Our previous analysis in Section 4.1 indicates that for networks with two cycles, the steady states are also unique. We also performed the same numerical experiment for the network in Figure 4 with only one cycle and the boundary data in Table 1. In Figure 8(a), we provide the resulting function H_p restricted to the corresponding root curve μ_η, which supports our previous observations. However, since we consider the mixture of two gases, our model has an additional equation, the mixing equation, and an additional variable, namely the mass fraction, which makes the proof of uniqueness more challenging.

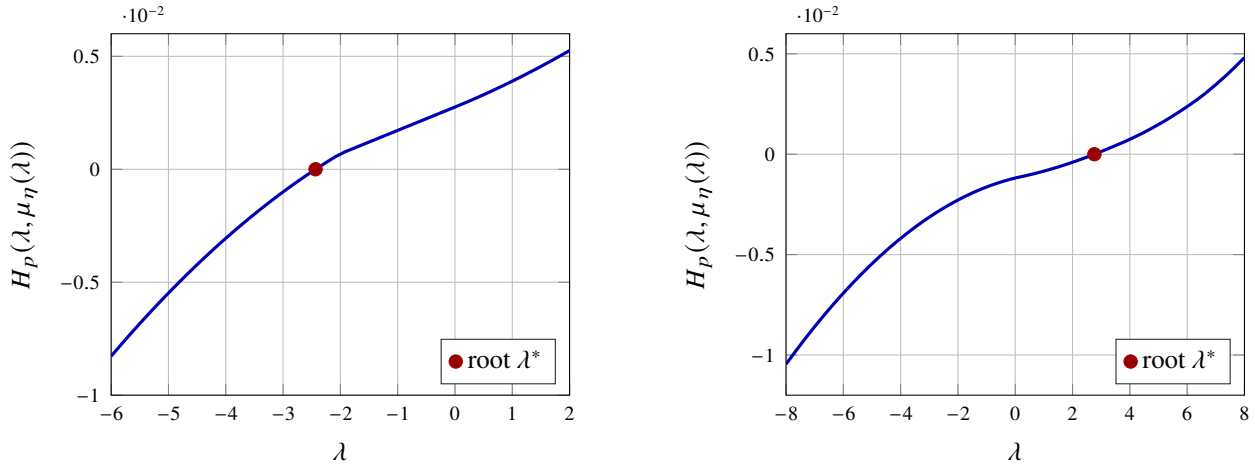

(a) Network with one cycle

(b) Network with two cycles

Figure 8. The function H_p restricted to the root curve $\mu_\eta(\lambda)$, resulting in $g(\lambda) = H_p(\lambda, \mu_\eta(\lambda))$.

The single gas result relies on the monotonicity properties of the flow q_e^c and the pressure p_e^c. The pressure increases with increasing nodal pressure and decreases with rising flow (cf. [29, Lemma 2]), while the flow increases with λ (cf. [29, Corollary 2]).

We prove that H_p is strictly increasing in λ by traversing from node v_{cr} to node v_{cl}, while applying Eq (2.4) and the "partial" monotonicity of the pressure and the flow. Since the authors consider only a single gas, μ and H_η do not appear in their analysis. Similar monotonicity properties hold for pressure and flow in the two-gas case, but establishing them with respect to λ requires additional information about the inflow and its effect on the mass fraction. Unlike for the pressure and flow, the monotonicity depends on the specific values of the composition of the gases, which becomes evident even for a simple example: Consider a node v with two incoming pipes e_1 and e_2 and one outgoing pipe e_3, where $q_{e_i} > 0$ for $i = 1, 2, 3$. Then, the nodal mass fraction at v is given by:

$$\eta_v = \frac{\eta_{e_1} q_{e_1} + \eta_{e_2} q_{e_2}}{q_{e_1} + q_{e_2}} \quad \Rightarrow \quad \partial_{\eta_{e_1}} \eta_v = -\frac{\left(\eta_{e_2} - \eta_{e_1}\right) q_{e_2}}{\left(q_{e_1} + q_{e_2}\right)^2}.$$

Hence, η_v increases with η_{e_1} if $\eta_{e_1} \geq \eta_{e_2}$, and decreases otherwise. Thus, we lack a "uniform"

monotonicity behavior, which leaves us unable to prove the monotonicity of H_p as of now. Nevertheless, numerical experiments, cf. Figure 8, suggest that $H_p(\lambda, \mu_\eta(\lambda))$ is monotonically increasing, making the uniqueness of steady states subject to future research.

5. Conclusions

In this paper, we have analyzed the steady-state problem of hydrogen-blended natural gas transport in pipeline networks. We have clarified the differences from pure natural gas transport and discussed the existence and uniqueness of solutions in networks. For tree-shaped networks, we can compute unique flows by the conservation of mass a priori, which guarantees the existence of a (unique) solution. For networks that include a cycle, we have applied an edge-cutting approach in order to show the existence of a solution. Cutting an edge in the cycle results in a tree-shaped graph with two new nodes and edges, and two additional coupling equations. We have shown that an admissible solution on the cut network exists, which also meets the two additional coupling equations. This implies the existence of a solution for the graph with a cycle.

The uniqueness of a solution for tree-structured networks follows by the fact that the flow direction is given a priori and thus, it is also clear a priori which node determines the composition on an edge. For networks including cycles, the composition of the gas on the edges in the cycle depends on the flow direction, leading to discontinuities in the mixing condition as discussed in Section 3.2. A natural extension of this work includes analyzing the discontinuities and thus also the uniqueness of a solution on networks with a cycle.

Additionally, considering optimization problems that involve hydrogen blends offers a valuable direction for future research. Such problems could explore the optimal blending ratios, operational settings, or cost efficiencies while ensuring safety and regulatory standards. Even though the simulation and numerical optimization results presented in [17, 20, 35–38] are promising, the research on the theoretical analysis of optimization problems that involve hydrogen-blended natural gas transport is still very limited.

Athors contribution

The authors A.U., M.S. and S.G. wrote Section 1. A.U. and M.S. wrote Section 2. A.U. wrote Sections 3 and 4. M.S. and S.G. wrote Section 5. A.U. prepared all figures. All authors reviewed the manuscript.

Use of AI tools declaration

The authors declare they have not used Artificial Intelligence (AI) tools in the creation of this article.

Acknowledgments

The authors thank the anonymous referees for their helpful comments that improved the overall quality of the manuscript. Furthermore, two of the authors were supported by the German Research Foundation in the Collaborative Research Center CRC/Transregio 154 (Mathematical Modelling,

Simulation and Optimization using the Example of Gas Networks), Project C03, Projektnummer 239904186 (Michael Schuster), as well as the grants GO 1920/11-1 and 12-1 (Simone Göttlich).

Conflict of interest

The authors declare there is no conflict of interest.

References

1. Bundesregierung, Energy from climate-friendly gas, 2024. Available from: https://www.bundesregierung.de/breg-en/news/hydrogen-technology-2204238.

2. *European Commission*, A hydrogen strategy for a climate-neutral Europe, 2020. Available from: https://energy.ec.europa.eu/system/files/2020-07/hydrogen_strategy_0.pdf.

3. *Office of Energy Efficienty & Renewable Energy*, Hydrogen: A clean, flexible energy carrier, 2017. Available from: https://shorturl.at/AjQv9.

4. *European Hydrogen Backbone*, Five hydrogen supply corridors for Europe in 2030 executive summary, 2022. Available from: https://ehb.eu/files/downloads/EHB-Supply-corridors-presentation-ExecSum.pdf.

5. K. Kumar, G. John, L. Lim, K. Seeger, M. Wakabayashi, G. Kawamura, Green hydrogen in Asia: A brief survey of existing programmes and projects, 2023. Available from: https://www.orrick.com/en/Insights/2023/07/Green-Hydrogen-in-Asia-A-Brief-Survey-of-Existing-Programmes-and-Projects.

6. *U.S. Department of Energy, OCED*, Clean energy demonstrations, mult-year program plan, 2023. Available from: https://www.energy.gov/sites/default/files/2023-08/OCED%202023%20Multi-Year%20Program%20Plan.pdf.

7. M. Banda, M. Herty, A. Klar, Gas flow in pipeline networks, *Networks Heterogen. Media*, **1** (2006), 41–56. https://doi.org/10.3934/nhm.2006.1.41

8. P. Domschke, B. Hiller, J. Lang, C. Tischendorf, Modellierung von gasnetzwerken: Eine übersicht, 2017. Available from: https://www.mathematik.tu-darmstadt.de/media/mathematik/forschung/preprint/preprints/2717.pdf.

9. T. Koch, B. Hiller, M. E. Pfetsch, L. Schewe, *Evaluating Gas Network Capacities*, MOS-SIAM, 2015.

10. M. Schmidt, M. Steinbach, B. Willert, High detail stationary optimization models for gas networks: Validation and results, *Optim. Eng.*, **17** (2016), 437–472. https://doi.org/10.1007/s11081-015-9300-3

11. M. Gugat, F. M. Hante, M. Hirsch-Dick, G. Leugering, Stationary states in gas networks, *Networks Heterogen. Media*, **10** (2015), 295–320. https://doi.org/10.3934/nhm.2015.10.295

12. M. Banda, M. Herty, A. Klar, Coupling conditions for gas networks governed by the isothermal Euler equations, *Networks Heterogen. Media*, **1** (2006), 295–314. https://doi.org/10.3934/nhm.2006.1.295

13. M. Gugat, S. Ulbrich, Lipschitz solutions of initial boundary value problems for balance laws, *Math. Models Methods Appl. Sci.*, **28** (2018), 921–951. https://doi.org/10.1142/S0218202518500240

14. E. S. Baranovskii, Feedback optimal control problem for a network model of viscous fluid flows, *Math. Notes*, **112** (2022), 26–39. https://doi.org/10.1134/S0001434622070033

15. M. Herty, Coupling conditions for networked systems of euler equations, *SIAM J. Sci. Comput.*, **30** (2008), 1596–1612. https://doi.org/10.1137/070688535

16. A. Quarteroni, L. Dede', A. Manzoni, C. Vergara, *Modelling Blood Flow*, Cambridge University Press, 2019, 25–76.

17. S. Kazi, K. Sundar, S. Srinivasan, A. Zlotnik, Modeling and optimization of steady flow of natural gas and hydrogen mixtures in pipeline networks, *Int. J. Hydrogen Energy*, **54** (2024), 14–24. https://doi.org/10.1016/j.ijhydene.2023.12.054

18. D. Bothe, W. Dreyer, Continuum thermodynamics of chemically reacting fluid mixtures, *Acta Mech.*, **226** (2015), 1757–1805. https://doi.org/10.1007/s00707-014-1275-1

19. J. Málek, O. Souček, A thermodynamic framework for heatconducting flows of mixtures of two interacting fluids, *ZAMM J. Appl. Math. Mech.*, **102** (2022), e202100389. https://doi.org/10.1002/zamm.202100389

20. P. Börner, M. Pfetsch, S. Ulbrich, Modeling and optimization of gas mixtures on networks, 2024.

21. A. Bermúdez, M. Shabani, Numerical simulation of gas composition tracking in a gas transportation network, *Energy*, **247** (2022), 123459. https://doi.org/10.1016/j.energy.2022.123459

22. M. Gugat, M. Schuster, Stationary gas networks with compressor control and random loads: Optimization with probablistic constraints, *Math. Probl. Eng.*, **2018** (2018), 7984079. https://doi.org/10.1155/2018/7984079

23. M. Schuster, E. Strauch, M. Gugat, J. Lang, Probabilistic constrained optimization on flow networks, *Optim. Eng.*, **23** (2022), 1–50. https://doi.org/10.1007/s11081-021-09619-x

24. S. Srinivasan, K. Sundar, V. Gyrya, A. Zlotnik, Numerical solution to the steady-state network flow equations for a non-ideal gas, *IEEE Trans. Control Network Syst.*, **10** (2022), 1449–1461. https://doi.org/10.1109/TCNS.2022.3232524

25. G. Guandalini, P. Colbertaldo, S. Campanari, Dynamic modeling of natural gas quality within transport pipelines in presence of hydrogen injections, *Appl. Energy*, **185** (2017), 1712–1723. https://doi.org/10.1016/j.apenergy.2016.03.006

26. A. Witkowski, A. Rusin, M. Majkut, K. Stolecka, Analysis of compression and transport of the methane/hydrogen mixture in existing natural gas pipelines, *Int. J. Press. Vessels Pip.*, **166** (2018), 24–34. https://doi.org/10.1016/j.ijpvp.2018.08.002

27. M. Gugat, J. Giesselmann, An observer for pipeline flow with hydrogen blending in gas networks: Exponential synchronization, *SIAM J. Control Optim.*, **62** (2024), 2273–2296. https://doi.org/10.1137/23M1563840

28. D. Wintergerst, *Optimization on Gas Networks under Stochastic Boundary Conditions*, Dissertation, FAU Erlangen-Nürnberg, Germany, 2019.

29. M. Gugat, R. Schultz, D. Wintergerst, Networks of pipelines for gas with nonconstant compressibility factor: Stationary states, *Comput. Appl. Math.*, **37** (2018), 1066–1097. https://doi.org/10.1007/s40314-016-0383-z

30. J. Bang-Jensen, G. Gutin, *Digraphs: Theory, Algorithms and Applications*, Springer London, 2008.

31. R. Bapat, *Graphs and Matrices*, Springer London, 2010.

32. C. Gotzes, H. Heitsch, R. Henrion, R. Schultz, On the quantification of nomination feasibility in stationary gas networks with random load, *Math. Methods Oper. Res.*, **84** (2016), 427–457. https://doi.org/10.1007/s00186-016-0564-y

33. S. Srinivasan, N. Panda, K. Sundar, On the existence of steady-state solutions to the equations governing fluid flow in networks, *IEEE Control Syst. Lett.*, **8** (2024), 646–651. https://doi.org/10.1109/LCSYS.2024.3394317

34. S. Srinivasan, K. Sundar, V. Gyrya, A. Zlotnik, Numerical solution of the steady-state network flow equations for a nonideal gas, *IEEE Trans. Control Network Syst.*, **10** (2022), 1449–1461. https://doi.org/10.1109/TCNS.2022.3232524

35. L. Baker, S. Kazi, R. Platte, A. Zlotnik, Optimal control of transient flows in pipeline networks with heterogeneous mixtures of hydrogen and natural gas, in *2023 American Control Conference (ACC)*, 2023, 1221–1228. https://doi.org/10.48550/arXiv.2210.06269

36. S. R. Kazi, K. Sundar, A. Zlotnik, Dynamic optimization and optimal control of hydrogen blending operations in natural gas networks, in *2024 Americal Control Conference (ACC)*, 2024, 5357–5363. https://doi.org/10.23919/ACC60939.2024.10644751

37. M. Sodwatana, S. Kazi, K. Sundar, A. Brandt, A. Zlotnik, Locational marginal pricing of energy in pipeline transport of natural gas and hydrogen with carbon offset incentives, *Int. J. Hydrogen Energy*, **96** (2024), 574–588. https://doi.org/10.1016/j.ijhydene.2024.11.191

38. M. Sodwatana, S. Kazi, K. Sundar, A. Zlotnik, Optimization of hydrogen blending in natural gas networks for carbon emissions reduction, in *2023 American Control Conference (ACC)*, 2023, 1229–1236. https://doi.org/10.48550/arXiv.2210.16385

AIMS Press